Sl. No.	IIT Ropar List of Recent Publications with Abstract Coverage: June, 2025
A	**Book Chapter(s)**
1.	A review on mechanisms of single-cell and collective cell migration: Insights into tissue dynamics **A Kiran, N Kumar, V Mehandia** -Mechanics and Materials Science of Biological Materials: Book Chapter, 2025 **Abstract:** Cell migration, whether occurring at the level of individual cells or as a collective effort, is a vital biological process shaped by the biochemical and biophysical characteristics of the surrounding microenvironment. In single-cell migration, movement is driven by actin-based protrusions, integrin-mediated focal adhesions, and actomyosin contractions, allowing cells to respond to environmental factors such as chemical gradients or substrate stiffness. On the other hand, collective cell migration involves the coordinated movement of interconnected cells within a monolayer, facilitated by structures like E-cadherin-based cell–cell junctions and the actin cytoskeleton. These intercellular interactions enhance the speed, directionality, and efficiency of migration compared to individual cells. Collective migration plays a pivotal role in maintaining tissue structure, remodeling, homeostasis, and in biological processes such as embryogenesis, morphogenesis, wound repair, and cancer metastasis. E-cadherin is crucial for maintaining mechanical stability, force distribution, and intercellular communication during collective migration, while its loss often triggers epithelial-to-mesenchymal transition (EMT), a critical step in cancer metastasis. Gaining a deeper understanding of the similarities and differences between single-cell and collective migration is key to unraveling the mechanisms behind tissue dynamics and disease development.
2.	Experimental technique and constitutive models for skin tissue: A review **KK Dwivedi, S Kumar, N Kumar** - Mechanics and Materials Science of Biological Materials: Book Chapter, 2025 **Abstract:** This review describes the characterization techniques and constitutive models which are used to measure and capture the structural and mechanical behavior of skin. Skin is nonlinear elastic, viscoelastic, and anisotropic material, and these mechanical properties of skin are subject-specific. The measurement of skin's mechanical properties differs among the experimental techniques [1]. One main cause of variability is the lack of standardization [2]. This chapter presents the mechanical and structural characterization methods that are widely used for skin research.
3.	Introduction to Google Earth Engine: A comprehensive workflow N Arora, S Singh, **V Sood**, DK Gupta - Google Earth Engine and Artificial Intelligence for Earth Observation: Book Chapter, 2025 **Abstract:**The basic requirement of each navigation system is to map the required dimensions onto a system and to simultaneously measure the important characteristics of a confined region. Google Earth Engine (GEE) is a cloud-based platform, providing planetary-scale geospatial analysis. GEE allows users to monitor various high-impact parameters such as wind speed, deforestation, water management, and climate monitoring. Monitoring these parameters allows the researchers to evaluate the climatic and observe the environmental change pattern, allowing them to develop prediction and rescue models for natural calamity prediction. The versatility of the software attracts a much wider audience apart from the researchers and is considered a boon for the audience that lacks the technical capabilities required to support a traditional

	supercomputer or a large-scale cloud computing resource optimization device.
4.	Investigating mechanical anisotropy of excised porcine skin using dog-bone specimen **P Lakhani, N Kumar** - Mechanics and Materials Science of Biological Materials: Book Chapter, 2025 **Abstract:** The natural alignment of the collagen fibers and its failure mechanics for the skin plays important in plastic surgery, dermatology, and forensic science. Skin is an anisotropic composite material made of elastin and collagen fibers along with ground substance. Effect of collagen fibers orientation on the mechanical properties and its failure mechanics was investigated in the present article. Custom-built uniaxial testing setup was developed for the quantification of the mechanical properties. Imaging technique was used for the measurement of the local strain distribution over the specimen surface. Dogbone shaped specimens were prepared in four different orientation parallel, 30°, 60° and perpendicular to the collagen fibers direction. Stress strain relations obtained from experiments were used for the calculation of mechanical properties like ultimate tensile strength, elastic modulus in toe region and linear region, transition point and strain energy absorbed before failure. Elastic modulus in the linear region, ultimate tensile strength and strain energy were higher for the parallel orientation of collagen. Scanning electron microscopy (SEM) images explains the role of collagen as the load bearing material. In the direction of collagen alignment fibrils fractured plastically and display flat failure. While perpendicular to the alignment direction fibrils were fractured and display a fringes pattern. Finally, finite element modeling (FEM) along with the imaging technique with the experiment was used to explain the role of specimen shape on the measurement of mechanical properties. In short, the present study explains the failure mechanics and provides the essential data and information for the modeling of skin for finite element simulation using anisotropic constitutive model.
5.	Mechanical characterization of hydrated and dehydrated goat bone **RN Yadav, N Kumar** - Mechanics and Materials Science of Biological Materials: Book Chapter, 2025 **Abstract:**The ability to determine the mechanical characterizations of bone at microscopic level has a great importance in biological and clinical application. Fatigue and static fracture generally occur due to repeated load or low intensity load for long term rather than trauma, most of the cases of fatigue failure is found in military, athletes, ballet dancer and in young children and frequently increases. The purpose of present study is to examine the mechanical properties of hydrated and non-hydrated bovine compact bone using nanoindentation technique. Here we examine elastic modulus, hardness, compressive and tensile strength and their viscoelastic nature by measuring storage and loss modulus of both grouped bones (Hydrated and non-hydrated).
6.	Multiscale assessment of bone fragility beyond bone mineral density **P Sihota, N Kumar** - Mechanics and Materials Science of Biological Materials: Book Chapter, 2025 **Abstract:** Recent research highlights that impairments in bone quality, rather than solely bone mineral density (BMD), are a significant factor in the weakened mechanical properties of bone seen in various medical conditions, including type 1 and type 2 diabetes, chronic kidney disease, cancer, and certain metabolic bone disorders. These conditions may alter bone quality without significantly affecting BMD, leading to an elevated risk of fragility fractures. Extensive studies have revealed that the BMD T-score, a widely used quantitative metric, frequently falls short in accurately predicting fracture risk. To address this, both in vivo and ex vivo methods have been utilized to assess bone quality, with a focus on structural, mechanical, and compositional characteristics. This review examines the multiscale evaluation of bone quality, emphasizing the key findings of different techniques and their respective limitations.
7.	Ultimate biomaterial: Titanium a gold standard choice for current orthopaedic implants

	M Sandhu, **N Kumar**, RS Sawhney, **J Jyoti,** K Singh, P Kaur - Mechanics and Materials Science of Biological Materials: Book Chapter, 2025 **Abstract:** Biomaterials are integral to numerous medical applications, encompassing orthopaedics, dentistry, medication delivery, tissue engineering, and cardiovascular devices. Ensuring biocompatibility, these materials must not harm the human body. They fall into four main classes: metals, polymers, ceramics, and natural materials, each with distinct properties and applications. Titanium alloys have emerged as preferred orthopaedic implant materials due to exceptional biocompatibility and mechanical properties, despite challenges like stress shielding and toxic elements. Advancements in beta titanium alloys offer improved biocompatibility, while shape-memory alloys present unique functionalities. Challenges such as nickel allergy persist, but ongoing research enhances biocompatibility and performance. In orthopaedics, implants are crucial for bone and joint repair, yet material-related failures prompt revisions. Factors like prosthesis design and surgical technique influence implant success, with titanium alloys often preferred for their fatigue strength. Strategies like surface coatings and ion implantation mitigate wear and friction issues. Biomaterials have evolved over four generations to address therapeutic needs, from bio-inert materials to bioactive and biodegradable substances. Fourth-generation biomaterials mimic natural tissues, coupling with electronic systems for advanced diagnostic and therapeutic applications. Classification into metallic, ceramic, polymeric, and composite categories aids understanding and application. Continued development holds promise for enhancing patient outcomes across medical disciplines.
B	**Conference Proceeding(s)**
8.	A comparative analysis and optimization of a distillation unit assisted Goswami cycle-absorption chiller assembly **A Singh, R Das** - National Conference on Multidisciplinary Analysis and Optimization, 2025 **Abstract:** The current study focuses on addressing the main weakness of the conventional Goswami cycle, namely that its cooling output is rather low in comparison to its ability to produce power. The suggested scheme incorporates a distillation unit assisted absorption chiller setup to the Goswami cycle, whose primary goal is to produce auxiliary cooling without any pressure losses and extra work input. The present modification has increased the conventional Goswami cycle's power and cooling output from 25.25 kW to 29.83 kW and 6.03 kW to 55.52 kW, respectively. Further, based on the assembly's thermal response and single objective optimization, it is found that its outputs from the Goswami cycle side, the absorption chiller side, and its exergy efficiency are in conflict with one other. After that, a multi-objective dragonfly algorithm and entropy-weighted TOPSIS methods are used to determine the optimal outputs for each side of the assembly at best possible exergy efficiency.
9.	A maximum mean discrepancy estimator enabled cyber attack detection in an autonomous AC microgrid **S De**, **R Sodhi** - 2024 23rd National Power Systems Conference (NPSC), 2025 **Abstract:**This paper presents a novel scheme to precisely identify cyber attacks, such as controller hijacking and unauthorized data modification, which can compromise an autonomous microgrid's (MG) frequency and voltage stability. The scheme is based on the Maximum Mean Discrepancy (MMD) index, which calculates the unbiased estimates of local voltage/frequency synchronizing tracking errors for each Distributed Energy Resource (DER). Under the compromised situation, MMD accurately and quickly distinguishes the attacked DER from the uncompromised DERs. The efficacy of the proposed cyber-attack detection scheme is tested under various types of cyber attacks on the IEEE-13 bus distribution feeder, modelled in RSCAD and is validated with Real Time Digital Simulator (RTDS) platform integrated with

	dSPACE1104 R&D automation controller through Hardware-in-the-Loop (HIL) simulation control environment.
10.	A variable duty cycle based method for high resistance connection fault detection in BLDC motor drives **A Gupta**, RS Reddy, **K Jayaraman** - 2024 IEEE International Conference on Power Electronics, Drives and Energy Systems (PEDES), 2025 **Abstract:**High-resistance connection (HRC) is a common issue in motor drive applications. These connections occur between the motor and inverter terminals, leading to voltage drops across the junction connectors and increased copper losses. HRC can create asymmetry in motor drive systems, degrading the motor's performance in terms of speed and torque. Therefore, reliable detection is crucial for implementing the mitigation techniques before the fault escalates and impacts the performance of the target application. This work proposes a new technique for detecting HRC faults in Brushless DC (BLDC) motor drives. In this technique, the DC link voltage across the motor terminals is varied for a fixed duration in an electrical cycle by adjusting the duty of the buck converter. This variation introduces a DC signal into the stator currents. By extracting the DC components from stator currents, it is possible to estimate the line resistances. Also, the severity of the fault is assessed using symmetrical component transforms. The proposed method is immune to variations in inductance and symmetrical variations in resistance. The above claims are supported by analytical expressions and experimental results obtained from a 36 V, 500 W BLDC motor drive.
11.	An improved Goswami cycle assisted by a distillation unit: A comparison and optimization study **A Singh, R Das** - National Conference on Multidisciplinary Analysis and Optimization, 2025 **Abstract:** This paper focuses on the conventional Goswami cycle, whose capacity to convert any waste heat source into useful outputs depends significantly on the quantity of vapor present at its turbine inlet. Clearly, any modification to increase the vapor generation will enhance the cycle performance. To achieve this, a distillation unit is added in the setup to generate additional vapor from the leftover working solution after the vapor extraction step in the conventional cycle. On comparing with the conventional setup, this modification has improved the total output/exergy efficiency from 31.28 kW/31.37% to 43.55 kW/32.68%, respectively. A single objective optimization is then performed on this modified setup, which reveals that it contains conflicting objectives. Based on this characteristic, a multi-objective dragonfly algorithm along with entropy-weighted *TOPSIS* decision method is used to obtain the best solution, which is 43.22 kW (turbine output), 10.54 kW (cooling output) and 31.48% (exergy efficiency).
12.	Decentralized frequency and DC-voltage deviation control in multi-terminal HVDC (MTDC) grids with high penetration of renewable sources AS Kumar, **BP Padhy** - 2024 IEEE International Conference on Power Electronics, Drives and Energy Systems (PEDES), 2025 **Abstract:**In the AC surrounded MTDC (AC-MTDC) grids, Frequency and DC-Voltage Deviation (FDVD) control are decisive for the system stability, and reliability. Accomplishing it through the decentralized manner while reducing interaction between droop controls is more exigent. To address this problem, FDVD based Adaptive Droop Control (FDVD-ADC) has been proposed in this paper. It adaptively changes Grid Side Voltage Source Converters (GS-VSC's), and Renewable Source side Voltage Source Converters (RS-VSCs) say Wind Farm VSC (WF-VSC) or Solar Farms VSC (SF-VSC) droop values based upon the deviation in frequency, and DC-voltage in the AC-MTDC grid. With the proposed method, renewable sources (like solar and wind farms) are also utilized to reduce FDVD in the AC-MTDC grid. To extract this support, these bulk solar and wind farms are operated in the Derated Mode of Operation (DMO). The

	simulation of the proposed method has been implemented on the CIGRE B4 DC benchmark model integrated into the two-area power system in PSCAD/EMTDC software. The efficacy of the proposed methodology is validated by comparing the traditional double droop control (PV2F) with the proposed method.
13.	Effect of simultaneous FDI and DoS attack of multi-area power system with dynamic event-triggering algorithm **S Beura, BP Padhy** - 2024 23rd National Power Systems Conference (NPSC), 2025 Abstract: The twenty-first century comes with advancements in information technology, which positively upgrades the conventional communication infrastructure. However, this improvement comes at the price of compromised system security. Broadly, the attackers can hamper normalcy in any system in two ways: firstly, falsifying data through the network in a false data injection (FDI) type attack; secondly, the attackers will make the network unavailable for communication in denial of service (DoS) attack. Lately, in a real-world scenario, the attackers are incorporating hybrid attacks, i.e., combining the above-mentioned attacks to damage the system performance further. The automatic load frequency control (ALFC) incorporated in modern smart grids relies on communication channels, so any interference in data can result in frequency diversion and instability in the system. Thus, a resilient H∞ controller, which is verified to be exponentially stable, designed by Lyapunov Krasovskii functional (LKF), is implemented in this work. The dynamic event-triggering algorithm (DETA) scheme is also incorporated with the controller to save on bandwidth use. The linear matrix inequality (LMI) method is used to find the controller's gain and weight of the event-triggered system of the three-area power system to verify the effectiveness of the designed controller.
14.	Efficient compression of PMU signal using Ramanujan's sum transform M Pandit, **R Sodhi** - 2024 23rd National Power Systems Conference (NPSC), 2025 **Abstract:**The Phasor Measurement Unit (PMU) forms the basis of a Wide Area Monitoring, Protection, and Control (WAMPAC) system. PMUs capture time-synchronized voltage and current phasors at a higher reporting rate of 50–60 samples per second using Information and Communication Technology (ICT) enabled Global Positioning System (GPS). This results in a significant amount of data that needs to be stored and transmitted for analysis in the control center. Therefore, an efficient PMU data compression scheme is necessary to reduce the cost of storage and the bandwidth required to transmit this data. In this paper, a simple PMU signal compression scheme consisting of 2 modules is proposed. Module 1 separates the event window from the steady state window using Statistical Variance (SV). This results in improved compression and reconstruction performance. Next, Module 2 compresses the separated windows using Ramanujan's Sum Transform (RST) method. The effectiveness of the proposed method is then compared with the conventional Discrete Cosine Transform (DCT) for various types of disturbances in the IEEE 14-bus system. Finally, the results demonstrate the effectiveness of the proposed method, while future direction is discussed at the end of the paper.
15.	Leveraging machine learning and self-administered tests to predict Covid-19: An olfactory and gustatory dysfunction assessment through crowdsourced data in India R Kumar, M Singh...**S Iyengar**, D Dash, R Kaur - International Conference on Cognitive Computing in Engineering, Communications, Sciences and Biomedical Health Informatics (IC3ECSBHI), 2025 **Abstract:** Olfactory and gustatory dysfunction are common manifestations associated with COVID-19 infection, typically identified through medical evaluations or self-reports. However, self-reports are often complicated by the common confusion between these senses. In this study, we explored whether practical smell and taste tests using household items could help assess these

	sensory losses. Participants completed an online survey, performing smell and taste tests with everyday items. We also collected demographic data, health. These authors have equally contributed to this work. information (including COVID-19 diagnosis), and current symptoms. Using various combinations of these factors, we built multiple random forest models to predict COVID-19 diagnosis. Incorporating data from the smell and taste self-tests enhanced the predictive accuracy of the models. Certain household items like clove for smell and lemon juice for taste demonstrated statistically significant capability in distinguishing infected ones from non-infected ones. This study demonstrates that simple smell and taste tests using household items can help predict COVID-19 infection, offering a potential home-based method to identify cases and limit transmission.
16.	Numerical and experimental investigation of freeform-fabricated auxetic structure-based planar mechanical metamaterial **S Singhal, R Kumar, S Marandi, A Agrawal, A Agrawal** - All India Manufacturing Technology, Design and Research conference, 2025 **Abstract:** The aerospace and automotive industries are working on lightweight structural materials with energy-absorbing properties and good mechanical properties to improve their functional parts' efficiency and fuel consumption. Using different foams and porous structure-based parts inevitably reduces the overall mass of carrier vehicles and parts. Due to its peculiar mechanical behavior (i.e., negative modulus and Poisson's ratio), specifically designed auxetic structure-based mechanical metamaterials have gained more research interest in recent years. It has resulted in the development of several new structural and hybridized unit cell-based auxetic structures with primitive, star, re-entrant, and origami-based structures. In the present work, an attempt has been made to design, simulate, and perform experimental characterization of re-entrant and star-based auxetic planar metamaterials for energy-absorbing applications. The designed structures are simulated using ABAQUS® with the ductile damage criterion to determine the failure modes under different loading conditions. The structures have been fabricated by acrylonitrile butadiene styrene (ABS) using the fused deposition modeling (FDM) process and further tested experimentally under compressive and tensile loading conditions. The digital image correlation (DIC) technique analyzes the strain field and calculates the Poisson's ratio of the designed structures.
17.	Orthopaedic implants-Ti based bio materials M Sandhu, **N Kumar**, RS Sawhney - International conference on circular economy and sustainable development (ICCESD-2024), 2025 **Abstract:** Over the past fifty years, a lot of research has been done on materials that the human body may use to create components that repair damaged bone structures. Ti-based materials offer the best possible balance of mechanical, chemical, and biological qualities, making them the most sought-after of all materials. The fields of traumatology, orthopaedics, and dentistry have confirmed the successful use of Ti biomaterials. Ti biomaterials have a comparatively low Young's modulus along with good strength. Although titanium has nearly the best level of biocompatibility among all metallic biomaterials, efforts are still being made to find novel ways to enhance both its biocompatibility and osseointegration. As a result, new alloys or composites made from chemically modified titanium open up new possibilities for the use of titanium in biomaterials. Additionally, a lot of focus has been placed on the nanostructure development in Ti-based biomaterials, which results in very good mechanical and biocompatibility qualities. Furthermore, Ti-based biomaterials' surface treatment promotes quicker osseointegration and, frequently, improves their mechanical qualities. The review focusses on the Orthopaedic Implants using Ti as a bio material.
18.	Performance analysis of active RIS-assisted full-duplex-two-way NOMA system under finite blocklength with hardware impairments

	S Kumar, B Kumbhani - 2024 IEEE International Conference on Advanced Networks and Telecommunications Systems (ANTS), 2025 **Abstract:**The active reconfigurable intelligent surface's (ARIS) potential of avoiding multiplicative fading loss by utilizing integrated reflection-type amplifiers has drawn considerable interest. This paper investigates the performance of ARIS-assisted full-duplex two-way (FDTW) non-orthogonal multiple access (NOMA) (ARIS-FDTW-NOMA) systems under finite blocklength (FBL) transmission regimes by using cascaded Nakagamim fading channels under hardware impairments (HIs). In this system, two users exchange their information simultaneously through NOMA with the help of ARIS. To assess the system performance, we derived the novel analytical expression of average block error rate (ABLER) and system throughput with the help of the Gauss Laguerre quadrature (GLQ) and Gauss Chebyshev quadrature (GCQ) method. Asymptotic analysis is also done at higher transmit power regimes to obtain useful insights. We have also compared the performance of the ARISFDTW- NOMA system with passive-RIS-FDTW-NOMA (PRISFDTW- NOMA) and ARIS-FDTW-orthogonal multiple access (ARIS-FDTW-OMA). Monte Carlo simulations are performed to verify the accuracy of the analytical expressions. Numerical results reveal that our proposed ARIS-FDTW-NOMA system outperforms PRIS-FDTW-NOMA and ARIS-FDTW-OMA scenarios in terms of ABLER and system throughput.
19.	Recent advances in plasma pyrolysis for plastic waste management A Sharma, A Kumar, **R Sharma**… - AIP Conference Proceedings, 2025 **Abstract:**Plastic waste management poses a significant challenge due to the material's durability and the volume of waste generated globally. Pyrolysis technology offers a promising solution by converting plastic waste into valuable products through thermaldecomposition. This review paper provides a comprehensive analysis of pyrolysis technology with a particular focus on plasma pyrolysis, a novel and advanced form of the process. Plasma pyrolysis utilizes high-energy plasma to achieve higher temperaturesand more efficient breakdown of plastic materials compared to conventional pyrolysis. The paper discusses the principles of pyrolysis, including the mechanisms, process conditions, and types of reactors used. Emphasis is placed on plasma pyrolysis, detailing its advantages such as reduced processing time, higher yield of desirable products, and lower emissions. Comparative analysis with traditional pyrolysis methods highlights the enhanced capabilities of plasma pyrolysis in handling mixed and contaminated plastic wastes. Challenges such as high energy requirements and system complexity are also addressed. The review concludes by identifying future research directions to optimize plasma pyrolysis technology, aiming to enhance its economic viability and environmental sustainability as a key component in global plastic waste management strategies.
20.	Transition and fault-tolerant scheme for single-phase inverter **PS Bhakar**, NBY Gorla, **J Kalaiselvi** - 2024 IEEE International Conference on Power Electronics, Drives and Energy Systems (PEDES), 2025 **Abstract:**Being a critical component of modern systems and in many machine-critical applications, reliability of power electronic converters, particularly inverters is of paramount importance. The reliability in single-phase inverter can be improved by employing redundant leg, module, etc. Redundancy (leg/module) utilises additional switches and connecting devices to provide fault tolerance for semiconductor faults. However, in a conventional fault-tolerant inverter, the redundant leg is inactive during normal/pre-fault operation, indicating the under-utilization of the redundant leg. Thus, the conventional fault-tolerant inverter needs to be modified to utilize the redundant leg in the normal as well as the post-fault conditions. This needs a highly effective transition scheme which can transform the usage of the redundant leg on

	occurrence of a fault. This paper investigates the potential timings of fault occurrence and their impact on the transition scheme. The detailed analysis is implemented and tested on the hardware prototype of a single-phase inverter.
C	**Journal Article(s)**
21.	Abenzothiazole-derived nanohybrid material tailored smart strip: A smartphone-assisted colorimetric kit for the quantification of spermidine levels in food samples K Kaur, Divya, S Kalra, N Kaur, **N Singh** - Journal of Agricultural and Food Chemistry, 2025 **Abstract:** Elevated levels of biogenic polyamines, specifically spermidine, have been linked to several foodborne diseases, thereby compromising global food safety and quality standards worldwide. It has also been recognized as a key biomarker for cancer diagnosis in early stages. Therefore, estimating spermidine levels is a crucial indicator in controlling foodborne illnesses. To address this, we propose a benzothiazole-based nanohybrid material, KK1–ZnO nanohybrid material + Cu(I), to analyze spermidine levels. The performance of KK1–ZnO nanohybrid material + Cu(I) toward detecting spermidine has been evaluated by a series of spectroscopic and electrochemical techniques. Further, a cost-effective, easy-to-use Smart Strip-based portable colorimetric kit has been proposed to visually analyze safe spermidine levels in food samples. This Smart Strip enables on-site detection and quantification of spermidine levels by comparing the Hue, Saturation, and Value (HSV) parameters for easy analysis. The pale-yellow strips coated with the KK1–ZnO nanohybrid material + Cu(I) turned greenish-blue upon exposure to spermidine. The Smart Strip kit offers different reference levels for easy comparison and quantification, thereby promoting human health and well-being. With this technology, one can easily assess spermidine levels in food samples, supporting healthier dietary decisions and overall well-being. 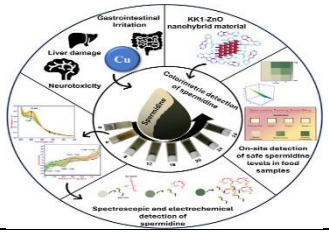
22.	A Comparative analysis of insertion of dental implants of V, square and trapezoidal screw designs **K Singh, R Upadhyaya,** M Rayes, S Bind, **A Poundarik, A Tiwari** - Next Research, 2025 **Abstract:** Approximately 3.5 billion people worldwide suffer from oral disorders, resulting in significant financial impact. In India alone, the impact is estimated to be USD 64 million. Approximately 54.7 % of patients are affected by peri-implant mucositis, according to prevalence rates. A study conducted by Friberg et al. (1991) reported a 32% failure rate in implants with inadequate initial stability. The achievement of primary stability is a prerequisite for the successful placement of dental implants. Appropriate implant designs have the dual advantage of supporting stability and promoting stress-induced bone adaptation in response to inadequate initial stability. This research employs finite element analysis (FEA) to model the detrimental effects of mastication stresses on the implant system to understand the stress dissipation and bone damage due to varied thread designs (V, Square, and Trapezoidal thread) on the human bone during an implantation procedure, by considering the implant as elastic-plastic material, which is not explored yet. Continuum damage mechanics using ductile damage is used in the research to understand the progression of damage in bone during the implantation procedure. Furthermore, a Ti-6Al-4 V dental implant is inserted into the bone with the use of progressive plasticity and continuum damage mechanics. In addition to evaluating stress distributions and energy dissipation over a range of threaded implant geometries, the friction coefficient between the implant and bone is integrated using a penalty technique. The numerical analysis provides

	information regarding bone damage caused by energy dissipation from different implant designs during implant insertion, an aspect previously overlooked in many studies. Results show that V-threads, with lower frictional and plastic dissipation energy, provide easier insertion and better initial stability compared to square and trapezoidal threads. This study suggests that using a combination of V-thread for initial insertion and square or trapezoidal threads for strength and bone engagement may optimize implant performance.
23.	A portable and power-efficient flue gas monitoring system for real-time air quality measurement **P Shukla, A Goel, V Kumar**, H Kaur, **VK Malav, B Rawat** - IEEE Sensors Journal, 2025 **Abstract:** In recent years, real-time monitoring of pollutants in flue gas emissions from industrial and transportation sectors has gained significant attention due to rising environmental concerns and the implementation of pollutant capture technologies. Despite these advancements, existing systems often fail to accurately measure pollutant concentrations in high-temperature flue gases with sufficient temporal resolution. To overcome these limitations, we present a compact and power-efficient flue gas monitoring system capable of simultaneously tracking 15 vital air quality parameters, including CO_2, O_2, particulate matter ($PM_{1.0}$, $PM_{2.5}$, $PM_{4.0}$, PM_{10}), temperature, humidity, VOC index, CH_4, CO, NO, NO_2, SO_2, and H_2S, with reliable spatial and temporal resolution. Central to the system is a modular pre-cooling unit, which reduces flue gas temperatures from approximately 150°C to within 30–45°C, enabling sensors to function optimally under thermal stress. To validate the robustness and discrimination capability of the system, field experiments were conducted by monitoring emissions from coal and torrefied biomass combustion in an industrialscale boiler. The results demonstrate that average CO_2 emission from coal combustion reaches approximately 618 ppm, which is 1.43× higher than those observed from biomass. Additionally, the power analysis of the system reveals an average current consumption of 0.0385 A, which can support the continuous operation for nearly six days using a 5000 mAh battery. The proposed system offers a scalable, cost-effective alternative to bulky commercial analyzers, with strong potential for deployment in industrial emission monitoring, environmental sensing, and smart infrastructure applications.
24.	ABCD parameter based analytical AC modeling of Novel Cu-carbon hybrid interconnects for noise constrained nanoscale systems B Kumari, M Sahoo, **R Sharma**- Scientific Reports, 2025 **Abstract:**A Copper-Carbon (Cu–Carbon) hybrid interconnect has been recently proposed for future VLSI applications, offering superior electrical performance compared to traditional interconnect structures. In the present era of high operating frequency, it is important to test this new structure for noise constrained applications specifically. In this work, ABCD parameter based analytical AC model of Cu–Carbon hybrid interconnects has been developed for efficient noise estimation in nanoscale systems. Several signal transmission parameters, noise parameters and frequency dependent complex conductivity and impedances of Cu–Carbon hybrid interconnects are estimated and compared with conventional copper (Cu) interconnects and emerging alternative copper-carbon nanotube (Cu-CNT) composite interconnects. The developed model is also verified with Advanced Design System (ADS) software. Cu–Carbon hybrid interconnects have the lowest impedance among other alternative configurations. Compared to copper, Cu–Carbon hybrid interconnect (with F_{cnt} =0.6) possesses ~80% lower impedance at 100 GHz frequency. Cu–Carbon hybrid experiences lowest return loss and highest forward transmission gain as compared to Cu and Cu-CNT composite interconnects. It demonstrates ~43% and ~48% lower S_{11} and ~30% and ~38% higher S_{21} values than copper at 100 GHz for single and 2-line coupled interconnects, respectively. At lower frequencies, all interconnects have comparable crosstalk noise profiles. The percentage improvement in the noise figure (in dB) and noise factor of Cu–Carbon hybrid is ~48% and ~98% at 100 GHz, respectively as compared with Cu interconnect. These analysis strengthens the claim of Cu–Carbon hybrid interconnect to be a worthier possibility for high frequency noise constrained applications in

	next-generation nanoscale systems.
25.	An efficient approach for parameter sensitivity analysis using sigma point method P Sehrawat, D Sarkar, S Kumar, **J Kumar** - Chemical Engineering Communications, 2025 **Abstract:** Parameter sensitivity analysis is being currently used in the modeling of physical phenomena in almost all engineering areas. The computational effort required to assess the importance of the uncertain parameters in a model is of utmost importance. In this article, a five-step process for parameter sensitivity analysis is proposed based on an efficient sigma point (SP) method. The SP method uses only $(2n+1)$ function evaluations for n number of uncertain input parameters. Several practical engineering problems, including two population balance models for the crystallization process of L-asparagine monohydrate and pyrazinamide, are evaluated to demonstrate the effectiveness of the proposed sensitivity approach. For the validation of sensitivity results obtained from the SP method, the polynomial chaos expansion (PCE) and optimal sparse PCE (OSPCE) methods are used as references. Before this, SP, PCE, and OSPCE methods are compared with the Monte Carlo simulations to check the accuracy of the three methods in approximating the mean and variance of the model outcomes. The results clearly indicate that the proposed SP-based sensitivity analysis approach is highly beneficial for complex dynamic models involving a huge number of uncertain parameters.
26.	Analogue information processing in NF-κB gene regulatory system **P Gautam, D Kashyap**, D Biswas, **SK Sinha** - Royal Society Open Science, 2025 **Abstract:** Nuclear factor-κB (NF-κB) participates in various cellular processes to encompass cell fate through differential gene expression, but the underlying molecular mechanism behind this phenomenon is still elusive. Two factors in this process can control the gene expression for determining the cell's fate: (i) synthesized proteins may have a considerable lifetime and (ii) gene activation may be slow or delayed. To address the first factor, we argue that the NF-κB system experiences cellular variability, often considered the origin of environmental noise for protein production, which influences cellular decisions at the molecular level as they have a considerable lifetime. We employ unified coloured noise approximation to obtain analytical expressions for the protein mean number obtained from our theoretical model and stochastic simulation. We find that these fluctuations influence mean protein numbers and induce bimodality. However, for the second factor, we rely on experimental findings, where the time delay in gene activation plays an essential role in protein production. Our bifurcation analysis demonstrates that the system exhibits saddle-node bifurcations for the instantaneous case, but it experiences the Hopf bifurcation and oscillates between two states in the presence of the time delay. In a nutshell, as NF-κB dynamics influence downstream expression, this study may provide insight into how to adjust parameters to control gene expressions.
27.	Analytical modeling of thiosemicarbazone metal complexes–based colorimetric array for high-throughput detection of multiple biogenic amines **H Singh, Ranbir**, G Singh, N Kaur, **N Singh** - Microchimica Acta, 2025 **Abstract:** A single polydentate ligand H6 was designed and synthesized using the azo-aldehyde as a colorimetric signaling unit and thiosemicarbazide derivative as a recognition unit. The concepts of combinatorial chemistry were implemented for the development of sensing elements of the array using a combination of single ligand H6 + multiple metallic cations (Cd(II), Cu(II), Ni(II), Zn (II), Na(I), and Ag(I)) and the array was utilized for the sensing of biogenic amines. Further, the effectiveness of the developed sensor array in distinguishing between analytes was assessed and compared using five distinct algorithms: principal component analysis (PCA), linear discriminant analysis (LDA), decision tree (DT), random forest (RF), and perceptron neural networks. The outcomes of principal component analysis concurred with the original hypothesis and established the discriminatory power of the array to detect multiple amines. Thereafter,

	classification of amines was performed using linear discriminant analysis and validated by leave-one-out cross-validation method, resulting in the remarkable accuracy of 98% when samples of varying concentrations were utilized, with detection limits in the range of 0.55–1.13 μM. Further, a combined principal component analysis and neural network (PCA + NN)–based algorithm was developed by using 6 PCA components as input of the neural network, having 3 hidden layers and 11 outputs for performing classification of biogenic amines. The PCA + NN algorithm outperformed all other methods and resulted in the maximum accuracy of 98.6% for successful classification of amines using the Adam optimizer and categorical cross-entropy as the loss function. Finally, the sensor array was successfully utilized for monitoring the quality of real chicken meat samples. 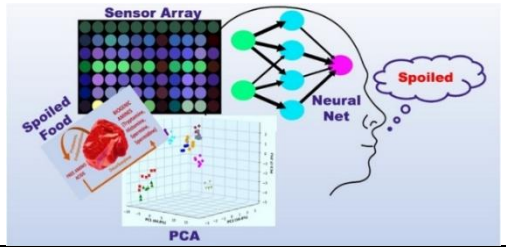
28.	Ancilla measurement-based quantum Otto engine using double-pair spin architecture **SR Rathnakaran, A Biswas** - Physical Review E, 2025 **Abstract:** We present a quantum-heat engine model utilizing a dual spin-pair architecture, wherein an Otto-like cycle is implemented using a single heat bath. The conventional cold bath is replaced by a measurement protocol, enabling engine operation without the need for a second thermal reservoir. Unlike standard quantum-heat engines, our framework employs an ancillary spin pair in a two-dimensional configuration to regulate performance. Operating in finite time, the engine attains finite power, which is enhanced through quantum correlations, specifically correlation between spin pairs and projective measurements on the ancillary pair. The system consists of dual-qubit pairs, where one pair serves as the working medium and the other as an ancillary system facilitating measurement-induced heat exchange. We demonstrate that the engine efficiency can exceed the standard quantum Otto limit through local control of the ancillary pair while maintaining nonzero power output. Moreover, correlation between spin pairs enables efficiency modulation via the measurement basis, underscoring the role of quantum resources in optimizing quantum thermal machines.
29.	Beyond the blade: A microstructural investigation of an ancient Indian steel sword **AK Patro**, K Venkatesh, S Prajapati, T Talapaneni, **PK Singh, A Lavakumar** - Metallography, Microstructure, and Analysis, 2025 **Abstract:** This study investigates a fourteenth-century sword from Kondapalli, India, revealing advanced ancient Indian metallurgical practices associated with crucible steels like Wootz. Optical emission spectrometry confirmed the blade as hypereutectoid steel (1.02 wt.% C), enriched with elements such as Si, Ni, P, and V. Multi-scale characterization (XRD, SEM, EPMA, and optical microscopy) revealed ferrite–cementite microstructures with distinct cementite bands aligned with microvoids containing silica-rich slag. Elemental segregation around these features suggests deliberate thermomechanical processing. The blade exhibited high hardness (~550–625 HV), while the ferritic hilt remained significantly softer (~158 HV), indicating functional material differentiation. The granular cementite morphology and selective coarsening, likely influenced by alloying elements, point to repeated forging cycles. These findings highlight sophisticated control over forging temperatures, deformation, and cooling, underscoring the metallurgical expertise of ancient Indian blacksmiths in optimizing performance through structural and compositional tuning.
30.	Bioinspired soft machines: Engineering nature's grace into future innovations AV Singh…**SK Samal**, P Malgaretti… - Journal of Functional Biomaterials, 2025

	Abstract: This article explores the transformative advances in soft machines, where biology, materials science, and engineering have converged. We discuss the remarkable adaptability and versatility of soft machines, whose designs draw inspiration from nature's elegant solutions. From the intricate movements of octopus tentacles to the resilience of an elephant's trunk, nature provides a wealth of inspiration for designing robots capable of navigating complex environments with grace and efficiency. Central to this advancement is the ongoing research into bioinspired materials, which serve as the building blocks for creating soft machines with lifelike behaviors and adaptive capabilities. By fostering collaboration and innovation, we can unlock new possibilities in soft machines, shaping a future where robots seamlessly integrate into and interact with the natural world, offering solutions to humanity's most pressing challenges.
31.	Candle soot/MXene incorporated robust superhydrophilic/underwater superoleophobic nanofibrous membrane for effective oil-in-water emulsion mixtureseparation K Thota, **M Sabapathy**, M Kakunuri - Colloids and Surfaces A: Physicochemical and Engineering Aspects, 2025 **Abstract:** Anthropogenic oil-related activities have significantly increased water pollution, posing a serious threat to the environment and human health. To address this challenge, innovative technologies for efficient oil-water separation are essential. In this study, a durable superhydrophilic and underwater superoleophobic ternary nanofibrous composite membrane was fabricated via electrospinning, utilizing polyacrylonitrile (PAN) as a polymer precursor embedded with hydrophilic candle soot nanoparticles and MXene layers. The inherent hydrophobicity of candle soot was modified to hydrophilic before incorporation into the polymer matrix. The structural morphology, wettability, thermal stability, chemical resistance, permeation flux, and separation efficiency of the ternary composite membrane were systematically investigated and compared with a binary composite membrane. The prepared ternary composite membrane achieves an underwater oil contact angle of $155 \pm 1.5^{\circ}$, significantly higher than the binary composite membrane's $130 \pm 1^{\circ}$. It also demonstrates superior water permeation flux of 3813 ± 81 L/m² h and separation efficiency of 99 ± 0.5 % for oil-in-water emulsion. For immiscible oil/water mixtures, a water permeation flux of 4468 ± 94 L/m² h and 99 ± 0.5 % separation efficiency were achieved solely through gravity-assisted separation. Additionally, the composite membrane retains over 96 % separation efficiency even after 15 cycles, demonstrating its durability through repeated use. 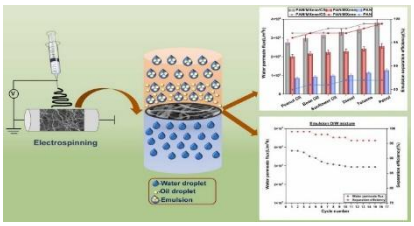
32.	ClipSwap++: Improved identity and attributes aware face swapping **PT Yee, S Mishra**, A Dhall - IEEE Transactions on Biometrics, Behavior, and Identity Science, 2025 **Abstract:**This paper introduces an efficient framework for an identity and attributes aware face swapping. Accurately preserving the source face's identity while maintaining the target face's attributes remains a challenge in face swapping due to mismatches between identity and attribute features. To address this, based on our previous work, ClipSwapclipswap, we propose an extended version, ClipSwap++, with improved model efficiency with respect to inference time, memory consumption, and more accurate preservation of identity and attributes. Our model is mainly composed of a conditional Generative Adversarial Network and a CLIP-based image encoder to generate realistic face-swapped images. We carefully design our ClipSwap++ with the

	combination of following three components. First, we introduce the Adaptive Identity Fusion Module (AIFM), which ensures accurate preservation of identity through the careful integration of ArcFace-encoded identity with CLIP-embedded identity. Second, we propose a new decoder architecture with multiple Multi-level Attributes Integration Module (MAIM) to adaptively integrate identity and attribute features, enhancing the preservation of source face's identity while maintaining the target image's important attributes. Third, to enhance further the attribute preservation, we introduce Multi-level Attributes Preservation Loss, which calculates the distance between the intermediate and the final output features of the target and swapped images. We perform quantitative and qualitative evaluations using three datasets, and our model obtains the highest identity accuracy (98.93%) with low pose error (1.62) on FaceForensics++ dataset and less inference time (0.30 sec).
33.	CMOA-Net: Competent multi-observant attention network for single-image super-resolution **Inderjeet, JS Sahambi** - IEEE Transactions on Emerging Topics in Computational Intelligence, 2025 **Abstract:** Recent advancements in deep convolutional neural networks show significant improvements in single-image super-resolution (SR). Existing SR methods typically focus on designing deeper or wider network architectures to enhance performance and fail to effectively utilize the low-resolution image features. However, these approaches often suffer from high computational costs. Additionally, several CNN-based methods face challenges in capturing adequate spatial context. We proposed the lightweight Competent Multi-Observant Attention Network (CMOA-Net) to address these issues and achieve more robust multi-scale features and feature correlations. The CMOA-Net includes an Efficient Feature Extraction Network (EFEN) that incorporates the Globalized Multi-Discerning (GMD) block and Competent Spatial Attentiveness (CSA). The proposed model is designed to enhance the representation capabilities of multi-scale features. Furthermore, The CSA module uses spatial and channel attention to capture long-range dependencies and preserve key features, enhancing output image quality. The effect of these combined components significantly enhances the proposed network performance, resulting in exceptional accuracy. Results reveal that the proposed state-of-the-art outperforms five synthetic benchmark datasets.
34.	Comparative analysis of deep learning and machine learning models for one-day-ahead streamflow forecasting in the Krishna River basin **S Kaur, SR Chavan** - Journal of Hydrology: Regional Studies, 2025 **Abstract:** Study region: Karad, Keesara, Sarati and T.Ramapuram catchments located in the Krishna River basin, India. Study focus: This study focused on 1-day ahead streamflow forecasting in four distinct catchments using a wide array of Deep Learning (DL) and Machine Learning (ML) models. A comprehensive evaluation of eleven models was conducted to assess their strengths and limitations across different datasets.New hydrological insights: The study implemented Long Short-Term Memory (LSTM), Bidirectional LSTM (Bi-LSTM), Gated Recurrent Unit (GRU), Bidirectional GRU, Convolutional Neural Network, WaveNet, K-Nearest Neighbours, Random Forest (RF), Support Vector Regression, Adaptive Boosting, and Extreme Gradient Boosting (XGBoost) to forecast streamflow at each site. Lagged precipitation and antecedent streamflow emerged as key predictors. Model performance was assessed using multiple evaluation metrics and visualization techniques. Bi-LSTM achieved the highest performance in three catchments with Nash-Sutcliffe efficiency (NSE) of 0.864 in Karad, 0.708 in Keesara, and 0.702 in T. Ramapuram, while GRU performed best in Sarati with NSE close to 0.7. The best model achieved "very good" accuracy in one catchment and "good" in three, as indicated by performance metrics. However, even the best-performing DL models struggled to capture peak flow events, revealing limitations in extrapolation. The study also highlights the potential of ML models based on ensemble techniques, such as RF and XGBoost, which demonstrated performance comparable to that of complex DL architectures.

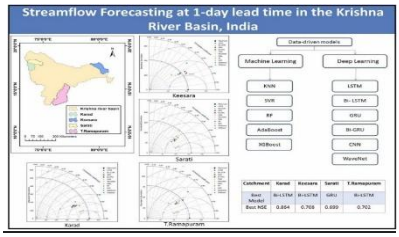

35. [Computational evaluation based case study of Schwarz-P TPMS lattice architectures for heat sink thermal performance]
SH Mian, CK Nirala, R Kant, U Umer - Case Studies in Thermal Engineering, 2025

Abstract: High-powered electronics are particularly vulnerable to the issue of increased failure brought on by excessive heat buildup. Intricately structured heat sinks, such as triply periodic minimal surfaces, have demonstrated capabilities, but their heat transfer performance are not yet fully understood. The goal of this study is to investigate the flow and heat transfer characteristics of the Schwarz-P heat sink via computational fluid dynamics. It evaluates the impact of unit cell size and porosity on the thermal performance of the Schwarz-P heat sink. The effectiveness of Schwarz-P-structure in relation to a plate-fin heat sink is also analyzed. The results indicate less tortuosity and that most of the fluid primarily flows through the central channel of the Schwarz-P heatsink. Flow separation is seen to be taking place when the fluid moves forward and confronts a change in the geometry. Flow reattachment and the development of recirculation zones are seen over a range of cross-sections. It is also noted that the thermal performance of the heat sink with the Schwarz-P structure has been enhanced compared to that of the plate-fin heat sink. This study is valuable as it outlines the relationships between the Schwarz-P heat sinks' design parameters and their thermal performance.

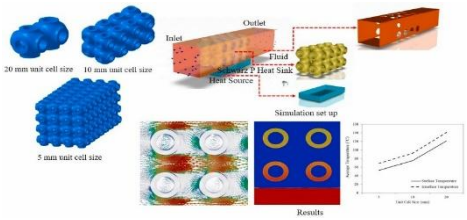

36. [Deflection of non-periodic ice sheet due to wave interaction in the presence of current]
A Aggarwal, SC Martha - Journal of Offshore Mechanics and Arctic Engineering, 2025

Abstract: A two-dimensional mathematical model for wave scattering induced by the interaction of a wave with a non-periodic variable ice sheet with the inclusion of current is presented, primarily focusing on the ice-sheet deflection arising from this interaction. The perturbation approach is initially used to solve the associated boundary value problem (BVP), followed by the Fourier transform technique. The main aim of this study is to derive an explicit analytical expression for the first-order deflection of the ice sheet and to examine its behavior for different physical parameters. Moreover, the surface strain of the ice sheet is also examined. For numerical simulations, an elastic plate having a Gaussian oscillatory shape is explored for its deflection under uniform current in connection to various physical parameters such as the spreading parameter, frequency parameter, and channel depth Froude number (current speed parameter). One significant observation is the emergence of an updrifting pattern in the deflection of ice sheet for very small spreading parameter values. In addition, the subharmonic peaks begin to transition into harmonic peaks as the Froude number increases. The findings of this study could potentially be useful to marine engineers and geologists while building coastal structures based on physical oceanographic conditions.

37. [Design methodology and analytical model for higher phase switched reluctance motor considering mutual coupling and saturation effect]

	Z Rayeen, S Payami - IEEE Transactions on Industrial Electronics, 2025 **Abstract:** The higher phase switched reluctance motor (HPSRM) (i.e., number of phases >3) is a potential candidate for industrial applications owing to its advantages of increased phase conduction overlapping. This leads to a higher power density and fault-tolerant capability with a reduced torque ripple. While designing a HPSRM, mutual coupling due to phase conduction overlapping between simultaneously excited phases should also be considered. However, when mutual coupling is considered in finite element analysis (FEA), the geometry optimization process and parametric analysis become computationally extensive and time consuming. This article proposes geometry parameter-dependent hybrid model of an HPSRM considering mutual coupling and core saturation, along with design approach. The design approach has minimal dependency on FEA for parameter optimization. Thus, the hybrid model and design approach significantly reduce the overall computation time with good accuracy. To demonstrate the effectiveness of the proposed model and design methodology, a 3-kW outer rotor five-phase switched reluctance motor (OR-FPSRM) is designed. The design parameters are optimized using genetic algorithm (GA) to achieve the desired output torque of OR-FPSRM. Analytical results obtained from the model are compared with those obtained through FEA using Ansys Maxwell and performance of the designed motor is also evaluated experimentally.
38.	Designing a sensor based on a π-conjugated 6-membered boron ring and its properties Z Zhang, **R Ahuja**, W Luo - Physical Review Materials, 2025 **Abstract:** Planar π-conjugated borides not only attract fundamental interests in bonding chemistry, but also offers wide-ranging applications in catalysis, bioimaging, and biosensing. To stabilize π-conjugated B_6 rings without out-of-plane bonding, we propose a design strategy that involves inserting low-compressible CN_3 triangles into tessellation of B_6 rings to create planar borides. Based on this concept, we designed the planar hypercoordinate boride ScC N_3B_6, which features the planar structure and represents a theoretically predicted π-conjugated B6 ring. The molecular dynamics simulations suggested that B_6 rings in ScC N_3B_6 remain intact at a high temperature of 1500 K. The metal adsorption energy of B_6 rings in ScC N_3B_6 is comparable to borophene, and superior to that of graphene and two-dimensional hexagonal boron nitride. As a result, the designed ScC N_3B_6 demonstrates both high stability and chemical activity attributed to CN_3 triangles and B_6 rings, respectively. Consequently, the designed ScC N_3B_6 could serve as a potential sensor for biomolecules. Moreover, the planar ninefold hypercoordinate Sc weakly bonds to the N_3B_6 wheel, drives a flat band of the dz^2 orbital, suggesting that flat band can be generated by splitting of dz^2 orbital in planar hypercoordinate crystal field.
39.	Durability assessment of ground granulated blast furnace slag-based CO_2 sequestered concrete K Saini, SK Saikia, **AS Rajput** - Journal of Sustainable Cement-Based Materials, 2025 **Abstract:** The emergence of CO_2 Sequestered Concrete (CSC) presents a promising avenue for mitigating net carbon dioxide (CO_2) emissions in the cement–concrete industry, thereby addressing climate change. The study focuses on evaluating the durability and microstructural attributes of CSC formulations incorporating Ground Granulated Blast Furnace Slag (GGBFS) as a supplementary cementitious material. Enhanced CO_2 sequestration was achieved through carbonation during mixing, curing, or both. The GGBFS-based CSC specimens, subjected to comprehensive evaluations of sequestration efficiency, mechanical performance, durability, and microstructural characteristics, demonstrated a 20% CO_2 uptake, a 19.9% increase in strength attributed to microstructural refinement, and a 29.4% reduction in chloride penetration, indicative of enhanced corrosion resistance due to reduced pore connectivity. These findings underscore the viability of CSC integrated with GGBFS as a sustainable solution aligned with global initiatives aimed at achieving carbon neutrality.
40.	Dynamic Strain Restoration During Plane Strain Hot Compression in Third-Generation γ-TiAl

	Alloys: Ti–45Al - (5, 10) Nb–0.2 C– 0.2 B **N Bibhanshu**, S Ranjan, A Bhattacharjee, S Suwas - Metallurgical and Materials Transactions A, 2025 **Abstract:** The influence of plane strain hot compression on dynamic strain restoration in third-generation gamma (γ) titanium aluminides, Ti–45Al – (5,10)Nb–0.2B–0.2C, was analyzed at 1150 °C and 0.1 s^{-1}. Microstructural analysis conducted before and after hot compression indicates that the alloy with increased Nb-content develops a higher proportion of dynamically recrystallized grains for 50 pct deformation. Additionally, kinking, breaking, and rotation of the α_2 and γ laths were identified that also contribute to the dynamic strain restoration. At 50 pct compression, Ti–45Al–10Nb–0.2B–0.2C shows a higher degree of recrystallization than the Ti–45Al–5Nb–0.2B–0.2C alloy. However, an increase in the deformation from 50 to 80 pct for Ti–45Al–5Nb–0.2B–0.2C led to a complete recrystallization for both phases with grown in their grain size. Ledge formation has been observed at the α_2–γ and γ–γ interfaces, potentially contributing to the strain relaxation. Low- and medium-angle grain boundaries were also found majorly in the region of remnant lamellae and the sign of recovery. Analyzed local orientation gradient formation between the phases shows that the α_2 phase equilibrates to higher strain; however, the γ phase releases its strain and shows a higher fraction of strain restoration. Further, strain restoration caused by dynamic recrystallization and deviation from the orientation relationship between the α_2 and γ phases were also characterized. 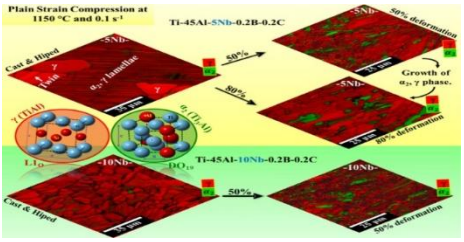
41.	Electrochemical functionalization of alkenes with 1, 3-Dicarbonyl compounds via radical addition **R Kumar, N Banerjee, S Pal, U Godara, P Banerjee** - Organic Letters, 2025 **Abstract:** Herein, an electrochemical approach for the functionalization of alkenes with 1,3-dicarbonyl compounds under oxidative conditions is reported. 1,3-Dicarbonyl compounds undergo single-electron transfer (SET) to generate electrophilic radicals, which upon addition to styrene and aliphatic alkenes afford the 1,2-bifunctionalized and α-alkylated products, respectively. The methodology avoids the usage of external oxidants and shows good tolerance with respect to alkene derivatives. 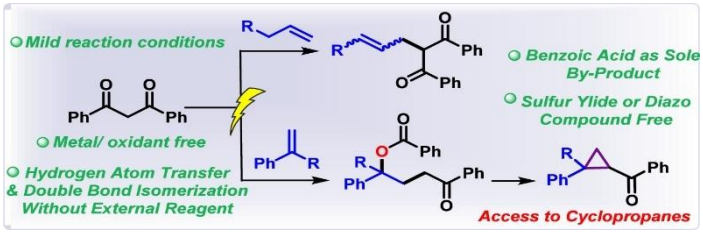
42.	Electrochemically reactive nanobubbles (ERNBs): An innovative solution for advanced oxidation processes (AOPs) in pollutant degradation and CO_2 utilization **G Yadav, P Koundle, H Sharma, N Nirmalkar** - Water Research, 2025 **Abstract:** Advanced oxidation processes (AOPs) play a crucial role in degrading persistent pollutants, disinfecting water, and treating industrial effluents. However, their widespread application faces challenges such as high energy consumption, low mass transfer, reliance on chemical reagents, lack of reaction sites, and the formation of toxic byproducts. Nanobubble

	(NB) technology offers an innovative solution by offering a high gas–liquid interface, enhanced mass transfer, and improved radical generation. This study investigates the application of electrochemically reactive nanobubbles (ERNBs) as a novel and effective strategy for AOPs, focusing on the degradation of persistent organic pollutants such as tetracycline (TC). The ERNBs, composed primarily of O_2 and H_2 NBs, were generated via water-splitting reactions at electrode surfaces. Their degradation potential was evaluated under varying operational parameters, including pH, electrolyte type & concentration, applied current, and initial pollutant concentration. Special emphasis was placed on the extended reactivity of ERNBs after generation, attributed to the formation of reactive oxygen species (ROS). The presence and role of ROS were examined using fluorescence spectroscopy, and the pollutant degradation mechanism was further elucidated through LC-MS-based identification of intermediates. In addition, the study explores the integration of CO_2 NBs as a sustainable alternative electrolyte, enabling simultaneous pollutant degradation and carbon utilization. The performance of ERNBs was validated in a complex synthetic wastewater matrix to assess their potential applicability in real-world scenarios. Overall, the findings support the development of ERNB-based AOPs as a promising and sustainable approach for wastewater treatment and environmental remediation. 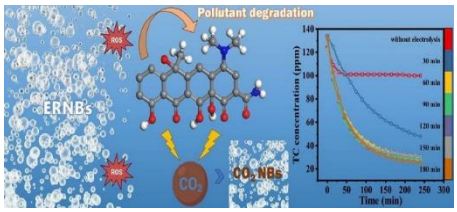
43.	Electromagnetic shielding with CFRP composites: Conducting matrix versus conducting fibers MK Srivastava, H Gupta, N Gupta, **PK Agnihotri,** S Basu - Polymer Composites, 2025 **Abstract:** Carbon fiber reinforced polymer (CFRP) composites are widely used in the aerospace industry. In order to render them opaque to incoming electromagnetic radiation, the current practice is to attach a thin woven or nonwoven metallic mesh with a suitable adhesive resin to the laminates. If the metal mesh is to be eliminated altogether, there are two competing strategies that can help increase the shielding effectiveness of CFRP laminates. Firstly, the isotropic electrical conductivity of the matrix can be improved by either adding conducting fillers or changing the matrix to one that is more conductive than epoxy. Secondly, the anisotropic conductivity of the individual carbon fibers or the carbon fabric can be improved. We conduct transfer matrix method (TMM) based simulations, considering a composite laminate to be an assemblage of anisotropic unidirectional fiber reinforced thin plies, with a view to assess the viability of these two strategies. Our results show that trying to enhance the longitudinal conductivity of the fibers is, by far, the more rewarding strategy. Finally, we conduct experiments on composites with carbon nanotubes dispersed in the epoxy matrix, and fibers with grafted nanotubes to reinforce the point. Using uni-directional carbon fibers grafted with carbon nanotubes, the total shielding effectiveness in the direction perpendicular to the fibers increased from ~20 to 30 dB and that along the fibers increased from 40 to 50 dB.
44.	Enrichment of aromatic hydrocarbon from hydrotreated light coker gas oil over a bimetallic zeolite catalyst B Joshi, S Singhal…**N Gopinathan**, O Singh, B Sarkar-ChemCatChem, 2025 **Abstract:** In order to address the crude-to-chemicals concept, it is imperative to transform low-value refinery streams into high-value petrochemicals. In this regard, the enhancement of aromatic hydrocarbons, particularly BTX from light coker gas oil (LCGO), is a critical step for future petrochemical complexes. A key aspect of this study was the development of a catalytic process to produce aromatics through successive hydrotreating followed by reforming of light coker gas oil (LCGO). A ZnCo-based bifunctional zeolite catalyst shows >73% paraffin conversion with 52.1% light aromatics selectivity. The study of the local structure and surface

	characteristics of the bimetallic catalyst reveals significant metal–support interactions, along with the presence of spinel phases in conjunction with ZnO and Co_3O_4. Additionally, ZnCo/ZSM-5 catalysts demonstrate superior acidity and an optimal balance of medium-strength Brønsted acid sites and high Lewis acid sites, which likely account for the improved BTX selectivity and reduced coke formation. 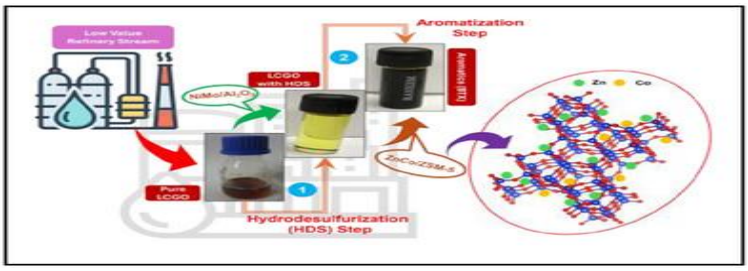
45.	European option pricing in regime switching framework via physics-informed residual learning **NK Pande, P Pasricha, A Kumar, AK Gupta** - Expert Systems with Applications, 2025 **Abstract:** In this article, we employ physics-informed residual learning (PIRL) and propose a pricing method for European options under a regime-switching framework, where closed-form solutions are not available. We demonstrate that the proposed approach serves an efficient alternative to competing pricing techniques for regime-switching models in the literature. Specifically, we demonstrate that PIRL eliminates the need for retraining and becomes nearly instantaneous once trained, thus offering an efficient and flexible tool for pricing options across a broad range of specifications and parameters.
46.	Examining barriers to solar energy adoption: A PESTEL and IVHF-DEMETAL analysis for advancing sustainable development goal 7 **T Pan, R Kumar**, CRH Foropon - Journal of Environmental Management, 2025 **Abstract:** This study presents a novel methodology for investigating the barriers that hinder the adoption of solar energy within an uncertain environment. To achieve the research objectives, the study first employs an analysis of political, economic, social, technological, environmental, and legal (PESTEL) factors, followed by the application of an interval-valued hesitant fuzzy decision-making trial and evaluation laboratory (IVHF-DEMETAL) approach. The IVHF methodology allows for the partial or complete consideration of uncertainties arising from expert doubts during the assignment of membership degrees in evaluations. An Influence-Dependence (I-D) chart has been plotted, which displays the overall hesitation of experts regarding all criteria, thereby enhancing the understanding of the findings. The results indicate that the most significant barriers to the adoption of solar energy systems are the ‘high initial capital cost’ and ‘insufficient commitment to government policies.’ This study provides valuable insights into the challenges faced by businesses and policymakers in transitioning to a sustainable energy system and in achieving the Sustainable Development Goals (SDGs), particularly SDG 7, which aims to ensure access to affordable and clean energy.
47.	Explicit and approximate solutions for the fragmentation equation in the presence of source and efflux terms: A coupled meshfree approach and its convergence analysis S Keshav, S Singh, Y Huang, **J Kumar**… - Kinetic and Related Models, 2025 **Abstract:**In this study, a novel coupled approach is presented for extracting analytical solutions of a fragmentation equation with source and efflux terms, specifically focusing on long time dynamics. This method holds significant potential in understanding complex phenomena such as polymer degradation (depolymerization), droplet break-up, grinding, and rock crushing in extended time frames. Obtaining analytical solutions for number density functions associated with complex structured Austin kernels remains a highly challenging and open problem. The series solutions are constructed using a semi-analytical Laplace decomposition method, followed

	by Padé approximation to extend the validity of the time domain. The detailed convergence is performed in order to enhance the understanding of the new approach using the Banach contraction principle. The new approach shows promising potential in finding series and even closed form solutions for the fragmentation equation with high precision, corresponding to analytically tractable and physically relevant kernels with various selection functions, starting from exponential and gamma initial distributions. In order to show the applicability of this approach, various numerical examples are considered and results are compared with the exact solutions or other numerical approximations (for kernels whose closed form solutions are not available). Remarkably, this method achieves the high accuracy by utilizing only a few series terms of the truncated form, and can be made uniform for all time if the limiting equilibrium distribution is known. Moreover, in the majority of cases, closed-form solutions for the number density functions associated with binary and multiple breakage kernels with different source and efflux terms are derived for the first time.
48.	Fabrication of Ti6Al4V alloy by wire arc additive manufacturing process and comprehensive machinability analysis **J Singla**, **N Kumar,** A Bansal, AK Singla, N Khanna - Wear, 2025 **Abstract:** Ti6Al4V alloy promises to have vide industrial applications owing to high strength, low density, and better resistance to corrosion. In the present study, in the first phase, Ti6Al4V alloy was fabricated by utilizing direct energy deposition techniques namely WAAM-CMT under controlled argon (approx. 99.9 %) environment with an aim to avoid oxidation. The WAAMed Ti6Al4V alloy showed 9.4, 19.14, 122.85, and 16.87 % higher ultimate strength, elongation, toughness, and microhardness, respectively as compared to wrought variant. This implies the suitable selection of WAAM-CMT process parameters along with proper protection under argon environment. Further, to evaluate its machinability, both the conventional and WAAM-CMT developed Ti6Al4V alloys have been subjected to drilling using TiAlN coated carbide twist drill bit under LCO_2 environment. The drilling performance parameters like tool wear, power consumption, cutting force, and torque have been assessed. Flank wear, thrust force, and surface roughness were found to be 94.17, 18.4, and 94.2 %. higher in the case of WAAMed alloy as compared to wrought alloy, respectively owing to its better mechanical properties as mentioned above. Due to improved mechanical properties like higher hardness for WAAMed alloy, the drilling tool gets blunt faster and the surface inside the hole becomes rougher with higher surface roughness as compared to the wrought alloy. Further, power consumption and torque seem to be independent of the flank wear with similar slight variations were reported for both the variants. The hole surface was found to be smoother in case of wrought alloy, which may correlate to its minimal surface roughness. Smaller chips were formed during drilling of WAAMed alloy, however, the macro aspects like curled shape seemed to be similar for both variants. Overall, it is recommended that Ti6Al4V components can be fabricated using WAAM-CMT under controlled argon environment. 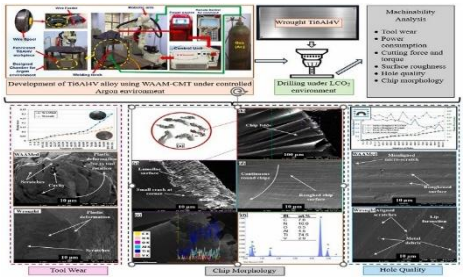
49.	First-order analysis of stromal collagen in chronic pancreatitis using cross-modality image translation with convolutional neural networks **Nisha, G Singhal, G Uppal, R Kumar** - Procedia Computer Science, 2025 **Abstract:** Chronic pancreatitis (CP) is a pancreatic disorder that involves persistent

	inflammation. The extracellular environment is primarily composed of fibrillar collagen with other matrix components. Collagen is excessively deposited during CP which leads to fibrosis, a hallmark of the condition. Second harmonic generation (SHG) microscopy allows for label-free, high-resolution and precise visualization of collagen structures and fibrotic changes at a microscopic level allowing accurate and quantitative assessment of the tissue microarchitecture. However, the need of specialized equipment and high costs associated with SHG microscopy limit its widespread use. This study aims to explore an image-to-image translation method using a convolutional neural network (CNN) architecture to generate SHG-equivalent 'collagen images' from H&E-stained brightfield (BF) microscopy images. The collagen images were generated through the image-to-image translation approach and the similarity of the translated images with SHG microscopy images was validated using multiple methods. The pixel intensity-based histograms of these translated collagen images were analysed using first-order texture analysis, revealing significant alterations in collagen texture associated with CP. Machine learning (ML) based models were utilized to assess and compare the classification performance of models. The performance of the collagen features for the optimal classification model was then evaluated through ROC-AUC (receiver operating characteristics – area under the curve) analysis. The proposed image-to-image translational approach can potentially provide a detailed and quantitative assessment of stromal collagen, improving the understanding of disease mechanisms and may further complement traditional histopathological workflow.
50.	Harnessing mesoporous g-C_3N_4-based photocatalytic materials for sustainable fuel production via solar energy conversion: a review P Dash, **AK Kar, R Srivastava**, K Parida - Materials Horizons, 2025 **Abstract:** The current energy production technology is associated with incompetent and unsustainable global conditions like climate change, the greenhouse effect, *etc*. Therefore, the call for sustainable and renewable energy practices is essential to address future energy crises, preserve ecological balance and combat climate change. Harnessing solar energy conversion *via* artificial photosynthesis over an efficient semiconductor is a key strategy to maintain the circular energy cycle and achieve zero-emission energy missions. g-C_3N_4 is one of the most exclusively studied semiconductor-photocatalysts; however, its bulk structure suffers from several significant limitations. Rational modifications of morphology and porosity led to the development of a mesoporous-C_3N_4 (mp-g-CN) framework, which has excellent photoresponsive features. mp-g-CN enriched with superior physicochemical properties, improved optoelectronic features, and well-dispersed active site distribution can be synthesized by either template-assisted or template-free synthesis methods. The template-free synthesis approach is more appealing than the template-assisted synthesis method, which can reduce the multiple synthesis steps and avoid the use of hazardous chemicals. Further, the strategic functional modifications deliver more efficient mp-g-CN structures, which can be considered as a reference photoactive material for producing H_2, H_2O_2, NH_3, carbonated fuel and biofuels from renewable precursors. Finally, some unresolved hitches in advancing mp-g-CN photocatalysts to achieve high efficiency in artificial photosynthesis have been encountered as current challenges and future prospects. 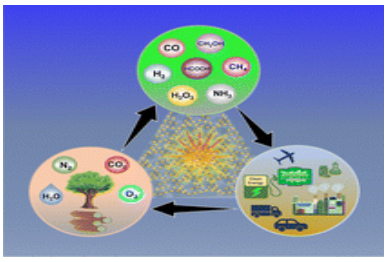
51.	Influence of build angles on layer characteristics at non-planar orientations during robot-assisted laser-wire DED **S Rathor, R Kant, E Singla, DK Goyal** - Progress in Additive Manufacturing, 2025

	Abstract: The build angles referred to as the wire feed angle (α) and substrate angle (θ) in additive manufacturing (AM), are essential for defining the multi-axis tool path and characteristics of bead geometry. This work fundamentally explores the influence of build angles on process physics, focusing on the bead peak shift and aspect ratio, to better understand laser-material interaction phenomena in the robotic non-planar laser-wire directed energy deposition (LWDED) process. The bead peak shift and aspect ratio are introduced for the first time in the context of optimizing build angles. A model based on laser-wire interaction (LWI) and incident angle for absorbed laser energy density has been introduced. The optimum build angles reveal that the wire feed angles are more significant in achieving improved results with an absolute error of 8.4% and 13.99% for the predicted aspect ratio and peak shift, respectively. The relationship between laser energy absorption and laser wire interaction volume has been developed. The optimized samples were tested for adhesion, scratch hardness, and microhardness. At an indentation load of 20 N, scratch hardness and microhardness strongly correlated for the optimum build angle sets. A non-circular laser beam shape, LWI time and pulsed laser influenced the characteristics of the bead during the non-planar LWDED process. These results help to achieve the required bead quality by deciding the build angles to facilitate automation in the LWDED process.
52.	Interface engineering and band alignment studies of Cu doped NiO as a hole transport layer for triple cationic perovskite solar cells **Puja, A Verma**, P Yadav, KS Nalwa, **M Kumar** - Small, 2025 **Abstract:** Hole selective inorganic transport layer plays an important role for higher stability of p-i-n perovskite solar cell. Here, this study investigates optimized Cu doping in NiO hole transport layer (HTL) and studied its interface with triple cation perovskite ($Cs_{0.05}(FA_{0.83}MA_{0.17})_{0.95}Pb(I_{0.83}Br_{0.17})_3$) absorbing layer. The optimized Cu doped NiO shows optical band gap of 3.17 eV with high electrical mobility and moderate carrier concentration of 43.2 cm^2/V-s and 1.51 × 10^{18} cm^{-3}, respectively. X-ray photoelectron spectroscopy analysis (XPS) shows modified Ni^{3+}/Ni^{2+} ratio with Cu doping in NiO, which enhances hole mobility and conductivity of HTL. The band alignment, recombination losses, and charge transport in several devices (FTO/Cu:NiO/$Cs_{0.05}(FA_{0.83}MA_{0.17})_{0.95}Pb(I_{0.83}Br_{0.17})_3$/Au) are also investigated using capacitance- voltage (CV) and electrochemical impedance spectroscopy (EIS). Optimized HTL showed a lower trap density (5.20 × 10^{20} cm^{-2} eV^{-1}), which resulted in a decrease of recombination losses and an increase in charge transport. The drift-diffusion model based simulation results also reveals the impact of interface defect density on power conversion efficiency (PCE). Final solar cell is fabricated on optimum Cu doped NiO HTL layers which showed an efficiency of 16.61% with enhanced fill factor (FF) of 77%. This study provides a detailed analysis of Cu doped NiO and their band alignment for a potential hole transport material in triple cation perovskite solar cells.
53.	Investigations on laser nitriding with trochoidal irradiation for enhancing corrosion resistance of laser-wire directed energy deposited low carbon steel **S Rathor**, A Kumar, **R Kant**, **E Singla**- Surfaces and Interfaces, 2025 **Abstract:** This study presents the process improvement in high-temperature surface nitriding using a lower pulsed laser beam and a trochoidal laser irradiation strategy. The trochoidal irradiation strategy is implemented for nitriding process improvement on heterogeneous laser-wire directed energy deposited (LWDED) low-carbon steel in a nitrogen gas atmosphere. The trochoidal path improves nitriding by overcoming the beam overlapping effect and uniform heating during laser interaction. The process mechanism reveals the petal-like structure on the processed surface, which creates a large surface area. This large surface area helps the nitrogen atom trap during surface melting to form a nitride surface. The intermediate diffusivity from a pulsed laser enabled the controlled nitride growth. It facilitated localized diffusion and the

	precipitation of the uniform Fe-nitride layer. The EIS analysis showed that the sample nitride at a laser frequency of 100 Hz has the best corrosion resistance in a 3.5 % NaCl solution. The higher-order Fe-nitride formation at 100 Hz frequency is retained after the corrosion test. This finding highlights the superior stability and durability of the 100 Hz laser frequency nitriding compared to the other samples. The effect of pulse frequency and trochoidal path on the formation of Fe-nitride is thoroughly investigated before and after electrolytic corrosion test using advanced characterization techniques like scanning electron microscopy, Raman spectroscopy, X-ray photoelectron spectroscopy, X-ray diffraction and electrochemical analysis. This study demonstrates the effectiveness of pulsed laser nitriding and a trochoidal strategy for enhancing corrosion resistance in additively manufactured parts. 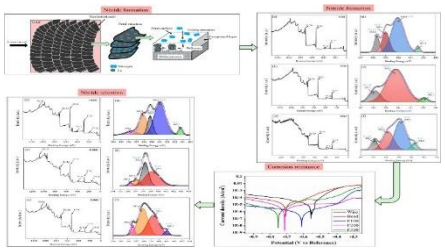
54.	Mechanical and electrical testing of encapsulated stretchable substrate interconnect models for emerging flexible electronic systems G Bhatti, Y Agrawal, V Palaparthy, **R Sharma**… - Microelectroconics Reliability, 2025 Abstract: Flexible electronics (FE) technology incorporates stretchable interconnects to enable devices those conform to irregular surfaces, bend and stretch without sacrificing functionality. These interconnects are crafted of specialized materials and designs those can withstand mechanical deformations with facilitating seamless integration of electronic components. Serpentine structures are widely used in flexible and stretchable interconnect. However, understanding their mechanical properties under different design parameters is crucial for optimal performance and reliability. In this work, through finite element analysis (FEA), the mechanical behaviour of serpentine interconnect structures with varying geometric parameters, along with and without encapsulation layer is novely investigated. The silver (Ag) material is used as conductor, while both substrate and encapsulation layers are formed using polydimethylsiloxane (PDMS). Also, the effect of mesh analysis is performed on the stretching of the considered interconnect models. Further, the Coffin-Mansons law based fatigue cycle test and the conductivity of the interconnect are analyzed. Finally, the simulation results are validated with experimental results. This research provides essential insightful observations on the interplay between design parameters, mechanical and electrical behaviour for the development of robust stretchable interconnect geometry in flexible electronic systems.
55.	Morph_CNeT: A new GIS tool to extract morphometric attributes characterising channel network topology of Indian catchments **S Rana, SR Chavan** - Journal of Hydrology: Regional Studies, 2025 **Abstract:** Study region: 21 River Basins comprising 1749 Catchments within India.Study focus: The morphometric attributes related to the channel network topology of a catchments are derived as functions of the emergence of the 1st, 2nd and 3rd bifurcation nodes of the network. These attributes are found to have influence on the shape of width function and hydrologic responses from catchments. There is a dearth of attempts to utilize these attributes in hydro-geomorphological applications, may be due to the complexity involved in their extraction owing to lack of any algorithmic procedure. This study is envisaged to develop an easy-to-use and time efficient Python based GIS code/tool named as Morph_CNeT within ArcGIS framework which provides an algorithmic way to extract the morphometric attributes.New hydrological insights for the region: Morph_CNeT is utilized to derive topological attributes for 1749 hydrological

	observation sites belonging to 21 river basins within India to build a repository titled "Morph_CNeT-India". Subsequently, the attributes are used to classify the catchments into several types of network topology as a function of the relative positions of first 3 internal nodes as well as their distances from the outlets. Finally, the empirical width functions constructed based on the morphometric attributes are shown to capture the multi-peaked behaviour of hydrographs to highlight significance of the attributes. The repository of morphometric attributes can form the basis for carrying out several hydro-geomorphological investigations. 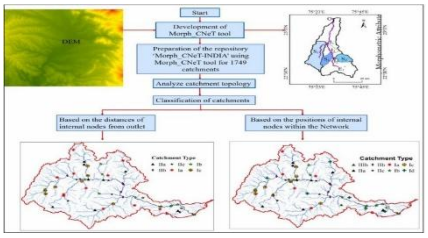
56.	π-Conjugated supramolecular self-assembled fluorescent sensor array for biogenic amines: A machine learning approach **U Kumar**, G Singh, N Kaur, **N Singh** - Organic Letters, 2025 **Abstract:** π-Conjugated supramolecular self-assembled fluorescence sensor arrays have been developed for the detection and discrimination of biogenic amines in food samples utilizing machine learning-assisted statistical algorithms such as principal component analysis (PCA), linear discriminant analysis (LDA), and hierarchical cluster analysis (HCA). The developed sensor array system is applied to the real-time and on-site detection of biogenic amines in food samples. Binary and ternary mixture analyses were successfully achieved. 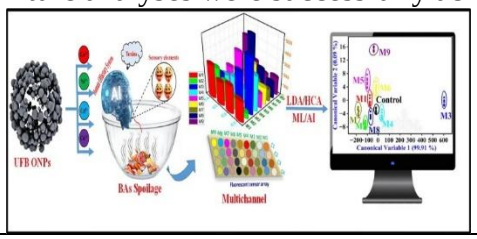
57.	Nanobubbles or impurities in alcohol-water mixture: Gas supersaturation mechanism and evidence **H Sharma, N Dutta, G Yadav, N Nirmalkar** - Journal of Molecular Liquids, 2025 **Abstract:** The debate on the presence of nanobubbles (NBs) in the alcohol-water mixture is an intriguing topic that has attracted interest in recent years. A major point of controversy regarding the formation of NBs in alcoholic solvents is the absence of auto-ionization. In this work, we hypothesize that nano-entities generated in alcohol-water mixtures are gaseous NBs rather than macromolecules/solid nanoparticles. Nano-entities were generated using the alcohol-water mixing method with varying volume ratios of methanol, ethanol, and isopropanol in water. The effect of O_2 sparging in alcohols and water before mixing was studied to investigate the impact of gas solubility on the generation of nano-entities. Ultrasonication was applied to the alcohol-water mixture to observe changes in the properties of nano-entities. Additionally, we present a mathematical model to estimate the work required for the nucleation of nano-entities, providing insight into the generation process. The concentration of generated nano-entities increased with the %v/v alcohol-water mixtures, peaked at a specific point, and then decreased, indicating the dependency on the gas supersaturation state. The refractive index (RI) estimation based on the Mie scattering theory shows that the generated nano-entities are most likely to be gaseous NBs, and their RI lies around 1.1-1.2 ± 0.06. Mixing of O_2-sparged alcohol with water increased nano-entities concentration, while ultrasonication of already prepared nano-entities suspension reduced their concentration, also giving indirect proof that the generated nano-entities are NBs.

	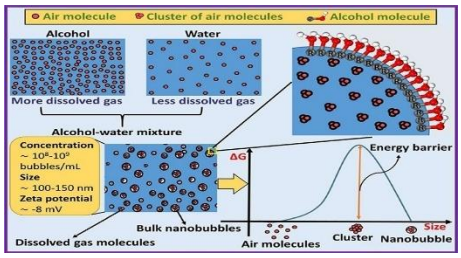
58.	Numerical investigation of fuel injection strategies for ammonia-diesel dual-fuel engine SA Karenawar, NK Yadav, **RK Maurya**, SAE Technical Papers, 2025 **Abstract:**This study numerically investigates ammonia-diesel dual fuel combustion in a heavy-duty engine. Detailed and reduced reaction mechanisms are validated against experimental data to develop injection timing maps aimed at maximizing indicated thermal efficiency (ITE) while mitigating environmental impacts using stochastic reactor model (SRM). The equivalence ratio, ammonia energy share (AES), injection timing, and engine load are varied to optimize combustion efficiency and minimize emissions. The results demonstrate that advancing injection timing reduces ITE due to heightened in-cylinder temperatures, resulting in increased heat losses through walls and exhaust gases. Maximum chemical efficiency is observed at an equivalence ratio near 0.9 but decreases thereafter, influenced by ammonia's narrow flammability range. Emission analysis highlights significant reductions in Global Warming Potential (GWP) and Eutrophication Potential (EP) with higher AES, driven by decreased CO2 and nitrogen oxides (NOx) emissions. Acidification Potential (ACP) initially rises with higher AES due to increased NOx production but diminishes as Pressure Rise Rate (PRR) and Ringing Intensity (RI) increase with higher AES and advancing injection timing. Conversely, Ozone Forming Potential (OFP) diminishes with higher AES due to reduced volatile organic compounds emissions.
59.	Observation of quantized spin wave modes in nano-constriction spin Hall nano-oscillators J Lei, S Zhao, **R Sharma**, Y Pu, F Hu, C Xu, H Yang - Applied Physics Letters, 2025 **Abstract:** Standing spin waves are crucial for advancing high-frequency spintronic devices and have been investigated using excitation methods such as cavity-based approaches, antenna-based techniques, and optical excitation methods. Unlike these conventional methods, we study quantized spin wave modes that satisfy the standing wave conditions across the nano-constriction in spin Hall nano-oscillators (SHNOs). We perform power spectral density measurements under various magnetic field conditions using Pt (6 nm)/$Co_{89.4}Gd_{10.6}$ (7 nm) SHNOs with constriction widths of 100 and 150 nm. In the SHNO with a constriction width of 150 nm, which is half of the wavelength of the spin wave, we observe two distinct spin wave modes: a propagating mode and a first-order quantized spin wave mode, the latter satisfying the standing wave confinement within the nano-constriction. Both modes are consistent with the Damon–Eshbach theory. Our findings demonstrate that geometric optimization enables the excitation of higher-order quantized modes at frequencies above the propagating mode, facilitating microwave signal generation at higher frequencies in SHNOs.
60.	On the general divisor problem of power moments of the coefficients attached to the dedekind zeta function over a sparse sequence NK Godara, **P Tiwari** - Results in Mathematics, 2025 **Abstract:** Let K_3 be a non-normal field of degree 3 over Q . Let l, K≥ 2 be two integers and $T_{K,}$ $K_3^{(n)}$ denotes the *k*-dimensional divisor function attached to the coefficients of the Dedekind zeta function in K_3. In this paper, we prove an asymptotic result for the following sum

	$$\sum_{\substack{n=x_1^2+x_2^2+x_3^2+x_4^2+x_5^2+x_6^2\le x \\ (x_1,x_2,x_3,x_4,x_5,x_6)\in\mathbb{Z}^6}} \tau^{\ell}_{k,\mathbb{K}_3}(n).$$
61.	Optimal and sustainable design of integrated biorefineries for microalgae and municipal solid waste processing A Elkamel, K Kim, F Hourfar**, MM Laljee**, M Fowler - Journal of Cleaner Production, 2025 **Abstract:** Increasing pressures on energy resources and the imperative to reduce greenhouse gas emissions are driving the exploration of alternative and viable energy sources. Biomass presents opportunities to produce a variety of valuable products including energy, chemicals, and materials. However, economic uncertainties arise from processing multiple biomass sources, and to address this issue, the current research covers a systematic framework for the optimal design of an integrated biorefinery through superstructure-based optimization, combining microalgae and municipal solid waste (MSW) processing pathways. A case study conducted for Seoul, South Korea—a city grappling with significant solid waste management and energy supply challenges—evaluates the economic feasibility of such an integrated biorefinery. Utilizing mixed-integer linear programming (MILP) in General Algebraic Modeling System (GAMS), the study identifies the optimal configuration for the biorefinery to maximize profitability. Results indicate that the proposed solution not only yields substantial quantities of valuable products but also reduces waste sent to landfills and enhances waste-to-electricity conversion. The end-products of the optimal configuration include all anticipated products except compost. The revenue from the sale of final products and the profit are $1.43 B/yr and $253.86 M/yr respectively for the optimal configuration obtained. Additionally, a sensitivity analysis assessing the impact of varying economic and feedstock conditions on the biorefinery's profitability and viability shows that the proportion of recyclable components in MSW has the biggest impact, followed by the market price of the biodiesel produced. The framework is generic as the superstructure can be modified in line with the requirements of the case at hand by selecting the appropriate feedstocks and technologies. Moreover, the relevant techno-economic parameters and equations can easily be incorporated into the mathematical model. Thus, this study has the potential to serve as a valuable decision-making tool for stakeholders when planning viable multi-feedstock biorefineries**.**
62.	Path connected dynamic graphs with a study of dispersion and exploration **A Saxena, K Mondal** - Theoretical Computer Science, 2025 **Abstract:**In dynamic graphs, several edges may get added or deleted in a round. There are different connectivity models based on the constraints on the addition/deletion of edges. One such model is the *T*-Interval Connectivity model, where edges can be added/deleted, keeping the graph nodes connected in each synchronous round. The parameter *T* depends on the stability of the underlying connected structure across rounds. There is another connectivity model, namely the Connectivity Time model, where the union of all the edges present in any *T* consecutive rounds must form a connected graph. This is much weaker than the *T*-Interval Connectivity as the graph may even be disconnected at each round. We, in this work, come up with a new connectivity model, namely *T*-Path Connectivity. In our model, the nodes may not remain connected in each round, but for any pair of nodesu, v, there must exist path(s) at least once in any consecutive *T* rounds. Our model is weaker than *T*-Interval Connectivity but stronger than the Connectivity Time model.We study the dispersion problem in our connectivity model. Dispersion is already studied in the 1-Interval Connectivity model. We show that the existing algorithm in 1-Interval Connected graphs for dispersion with termination does not work in our *T*-

	Path Connectivity model for obvious reasons. We answer what are the necessary assumptions to solve dispersion in our connectivity model. Then, we provide an algorithm that runs in optimal time with those minimal model assumptions on *T*-Path Connected graphs. Also, we show that solving dispersion is impossible in the Connectivity Time model, even in the presence of several other strong model assumptions. Further, we initiate the study of the exploration problem on these three connectivity models. We provide several impossibility results with different assumptions. In most cases, we establish necessary and sufficient conditions to solve the exploration problem using an optimal number of agents in an asymptomatically optimal time. It is also evident from the studies of dispersion as well as exploration on all the three connectivity models that, Connectivity Time model is indeed the weakest model among these three models.
63.	Post-Annealing effect on microstructure, crystallinity and scratch resistance of baghdadite coatings with CNT inclusions by plasma spraying **S Singh**, D Sharma, **H Singh**, **K Rakha** - Ceramics International, 2025 **Abstract:** Heat treatment is a well-known approach to enhance both the mechanical and biomedical characteristics of thermal sprayed coatings. This study focused on the deposition of pure baghdadite and baghdadite coatings reinforced with carbon nanotube onto titanium substrate using a plasma spray technique. The coatings were annealed in a tube furnace at 400 °C, 600 °C, and 800 °C, and their effects on microstructure, phase crystallinity, hardness, and scratch resistance were thoroughly investigated. XRD results have indicated that crystallinity has been highest at 800 °C, suggesting that increased annealing temperatures have promoted phase transformation. Raman spectroscopy has shown an increase in G-band intensity at 800 °C in Baghdadite coatings with CNT inclusions coatings. Porosity and surface roughness measurements have revealed that higher annealing temperatures have led to increased densification and smoother surfaces, enhancing coating uniformity. Microhardness testing has demonstrated a significant improvement with annealing, particularly at 800 °C, due to the reduction in porosity and defects within the coating. Scratch testing results have shown reduced penetration depth, lower wear volume loss, and enhanced scratch resistance at higher annealing temperatures. The BAG-CNT coatings have exhibited superior mechanical performance compared to pure BAG coatings under all annealing conditions. At 800 °C, the scratch wear rate for BAG and BAG-CNT coatings has been reduced by 33.11 % and 31.94 %, respectively, as compared to 400 °C. The primary failure mechanisms observed in the coatings have included material chipping, micro-cracking, and spallation.
64.	Power efficient and long range precision agriculture monitoring system **R Raina, KJ Singh, S Kumar** - IEEE Journal of Radio Frequency Identification, 2025 **Abstract:** Precision agriculture, also referred to as precision farming or smart farming, uses technology to improve the efficiency, sustainability and productivity of agricultural practices. Traditional precision agriculture systems often suffer from limited communication range and high power consumption, which restrict their scalability and long term deployment in large scale farms. Furthermore, existing literature lacks integrated solutions that address both range extension and power minimization in precision agriculture monitoring. To bridge this gap, multiple power efficient soil moisture monitoring nodes are deployed in the farm which transmit data using Bluetooth Low Energy (BLE) technology. Also, this paper investigates the power consumption of the entire precision agriculture monitoring system, including both the sensor nodes and the gateway, which has not been addressed in the previous research works. Soil moisture node has a battery lifetime of 114.18 hrs with 620 mAh / 3V battery. The soil moisture data is received by the gateway (receiver) which then sends data to the cloud. Also, Low Noise Amplifier (LNA) is used at the receiver which reduces the packet loss and increases the range of soil moisture monitoring nodes. Additionally, light intensity (VCNL4040), anemometer, temperature and humidity (SHT40) sensors are interfaced with the gateway which sends data to the cloud directly using Global System for Mobile Communication (GSM) technology.

	Therefore, this paper proposes novel and power-efficient agricultural monitoring device that also acts as a gateway has a battery life of 106.74 hrs with 15600 mAh / 4.2 V battery. Additionally, the mean absolute errors calculated for the soil moisture sensor (ZSSC3123), VCNL4040, SHT40 and anemometer using reference sensors are 0.1, 1.9, 1.33 and 1.42 respectively.
65.	Predicting jams in heterogeneous disordered Traffic: Insights from tipping point theory **SN Chattopadhyay, AK Gupta** - Applied Mathematical Modelling, 2025 **Abstract:** Regime shifts, characterised by abrupt transitions, occur widely in complex systems, from ecosystem collapses and marine ice instability to traffic congestion and disease outbreaks. Statistical indicators with universal applicability, known as early warning signals, are key for predicting such critical transitions in advance. This study introduces an intriguing lattice hydrodynamic area occupancy model, incorporating vehicular passing effects, to explore the dynamics of heterogeneous traffic systems typical of emerging economies, where infrastructural constraints and a lack of lane discipline increase traffic complexity. The formation and evolution of kink and chaotic traffic jams are analysed through theoretical modelling and numerical simulations. A systematic framework employs generic statistical measures - including standard deviation, skewness, kurtosis, and lag-1 autocorrelation - to identify early indicators of impending congestion. A comprehensive sensitivity analysis of the indicators' processing parameters and evaluations of their significance and robustness are performed to ensure a more nuanced and insightful interpretation. Results reveal that the statistical measures' predictive performance is sensitive to the choice of moving window size and bandwidth of the smoothing function. Further, it is observed that the higher-order moments are more prone to yielding false negatives, irrespective of the traffic jam being kink-antikink type or chaotic. This work provides a robust basis for predictive methodologies to address congestion in highly heterogeneous environments, offering insights into the interplay between statistical indicators and phase transitions in complex transportation systems.
66.	Progression and natural history of Atypical Parkinsonism (ATPARK): Protocol for a longitudinal follow-up study from an underrepresented population R Yadav, S Dey…, **DRBathula** - PloS one, 2025 **Abstract:** Background: Atypical Parkinsonian Syndromes (APS) form the third largest group of neurodegenerative disorders including Progressive Supranuclear Palsy (PSP), Multiple System Atrophy (MSA), and Corticobasal Syndrome (CBS). These conditions are characterized by rapid progression, poor prognosis, low survival rates, and limited treatment options. Few studies have suggested that genetic, environmental factors and inflammation contribute to the pathobiology of these complex disorders, however, the etiology of disease and progression remains unclear.Methods: A multicenter prospective longitudinal (3-time point) study will be conducted with a total sample size of 400 across all the groups (PSP, MSA, CBS). Patients with APS will be recruited after a detailed evaluation by movement disorder specialists and obtaining valid informed consent. The socio-demographic data and whole exome sequencing will be performed only at the baseline. Non-invasive procedures such as neurological and cognitive assessments, sleep quality assessments including polysomnography, brain imaging, and retinal imaging will be conducted at each time point. In addition, gene expressions, methylation patterns, inflammatory cytokines, disease-associated pathological proteins (Tau, pTau-181, α-synuclein and β-amyloid), non-targeted proteomics, skin biopsy, and iPSC will be performed at each time point eventually. The statistical analysis will be performed, followed by the developing of machine learning (ML) models.Expected outcomes and conclusion: This unique native dataset in APS will enhance our understanding of the molecular mechanisms driving pathological protein aggregation and disease progression. Furthermore, the longitudinal design of the study enables a detailed examination of symptom development, progression, and management. The ML models combined with advanced imaging techniques will aid in early diagnosis, differentiation among APS types, and the development of future clinical trials and treatment strategies.

67.	Reconstruction of the 2023 South Lhonak Lake outburst flood and modelling future scenarios in the Sikkim Himalaya **D Gaikwad, RK Tiwari**, A Goswami - Natural Hazards, 2025 **Abstract**: On October 4, 2023, a catastrophic Glacial Lake Outburst Flood (GLOF) occurred from South Lhonak Lake, located in Sikkim, Himalaya. This resulted in large-scale destruction, which included the failure of the 1200 MW Teesta III dam. In addition to the GLOF, simultaneous occurrence of heavy rainfall exacerbated the flooding across the state. Therefore, based on remote sensing data, this study aims to reconstruct this extreme flood event to assess flood discharge contributions from both GLOF and rainfall using hydrodynamic and hydrological modelling using HEC-RAS and HEC-HMS, respectively. The simulation of the actual GLOF event revealed peak discharges of ~7355 m^3/s at Chungthang and ~8282 m^3/s at Gazoldoba. The calibration of hydrological simulation agreed with available observed streamflow data at Gazoldoba showing the peak discharge of ~8252 m^3/s, obtaining accuracy of 78%. Additionally, three potential future re-outburst scenarios of South Lhonak Lake were also modelled: (1) considering its current size, (2) triggered by a GLOF from the upstream North Lhonak Lake, and (3) considering potential future lake expansions. Correspondingly, the modelled peak discharges at Chungthang for these scenarios were 8826 ± 1015 m^3/s, 10817 ± 1244 m^3/s, and 12385 ± 1424 m^3/s, respectively. Thus, this study underscores the utility of integrated models in capturing the complex meteorological and hydrological characteristics of extreme flooding events driven by multiple hazards. The findings offer critical insights that are essential for developing effective flood risk management and mitigation strategies in glacial lake-dominated regions.
68.	Role of support in phenol hydrodeoxygenation over supported Pd catalysts: Insights from first-principles based microkinetic modelling **DR Kanchan, A Banerjee** - Journal of Catalysis, 2025 **Abstract:** Catalytic Hydrodeoxygenation (HDO) of biomass pyrolysis-derived bio-oil is a critical step for reducing oxygen content in the bio-oil, before its utilisation as a fuel. In this regard, HDO of bio-oil model compounds have been investigated over numerous supported metal catalysts, but the role of support on the catalytic activity has been largely ignored. In this work, the reaction mechanism for HDO of phenol – a bio-oil model compound was investigated on Pd/Al_2O_3, Pd/ZrO_2 and Pd/TiO_2 catalysts. Comprehensive reaction map and energetics of the multiple reaction pathways for phenol activation to benzene and cyclohexanone were elucidated using first-principles Density Functional Theory (DFT) calculations. The metal-support interface provides a unique site for the adsorption of the reactants and the intermediates, which alter the reaction mechanism and consequently the product distribution. Over TiO_2 and ZrO_2 supports, phenol adsorbs on the Pd-support interface with the phenolic O binding to oxophilic cation of the oxide support and ring carbon to Pd, thereby weakening the C_{aryl}-O bond and facilitating its cleavage to form benzene. In the case of Al_2O_3, phenol adsorbs only through the ring carbon on the Pd, which results in ring-hydrogenated products like cyclohexanone. A microkinetic analysis revealed the direct deoxygenation pathway to benzene to be favoured over Pd/ZrO_2 and Pd/TiO_2, while cyclohexanone production via a phenoxy intermediate was favoured on Pd/Al_2O_3, in agreement with experimental results. 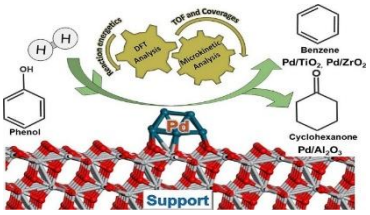
69.	Selective upcycling of aromatic polymer waste into light C_6-C_9 aromatics over Ru-supported catalysts

	AK Manal, J Zhao, R Bal, **R Srivastava**-ChemSusChem, 2025 **Abstract**: The valorization of plastic waste and biomass has gained significant attention in the twenty first century. Despite structural similarities and the potential to yield similar products, an integrated approach to converting both feedstocks using the same catalyst has not been realized. This study demonstrates the catalytic upcycling of plastic waste and lignin biomass into selective C_6-C_9 aromatics through C-O and/or C-C bond cleavage using Ru-supported catalysts. The Ru/TiO_2 exhibits remarkable performance, achieving 75%–90% yield from single, mixed plastic polymers and lignin. The exceptional activity of Ru/TiO_2 stems from its unique structural and electronic properties. H_2 spillover at the Ru–TiO_2 interface transfers in the form of H^+/e^-, where the e^- reduces TiO_2 to TiO_x, generating surface oxygen vacancies and inducing strong metal support interactions, while H^+ migrates to the adjacent oxygen sites, forming new Brønsted acid sites. Oxygen vacancies at TiO_x sites promote the activation and cleavage of C-O bonds, while Brønsted acid sites assist in the cleavage of C-C bonds. Additionally, ultrasmall, highly dispersed Ru suppresses the hydrogenation of aromatics. These synergistic properties enable Ru/TiO_2 to selectively produce aromatics, offering a promising strategy for catalytic upcycling of aromatic polymer waste into sustainable chemicals, aligning with the circular economy. 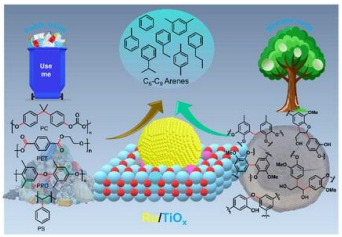
70.	Synergetic study of Al_2O_3-boric acid in copper matrix: Aluminum borate formation and its effect on tribological characteristics of copper-based composites RKS Gautam, P Jha, JK Gautam**, H Nautiyal**, S Singh, RN Goswami, R Tyagi - Wear, 2025 **Abstract:** The current research work involves the microstructure, mechanical and tribological performance assessment of copper-based composites developed by powder metallurgy (PM) route, namely Cu-4wt.% Al_2O_3 (CAB0), Cu-4wt.% Al_2O_3-2wt.% H_3BO_3 (CAB2) and Cu-4wt.% Al_2O_3-4wt.% H_3BO_3 (CAB4) in extended working regime of loads 4, 6, 8 and 10 N at a constant sliding speed of 0.05 m/s. The abbreviation CAB define the Cu matrix, alumina and boric acid accordingly based on the wt.% of boric acid in the hybrid composites CAB0, CAB2 and CAB4 has been designated in the current study. During the tribo tests, GCr15 steel ball (φ 6 mm) was selected as a counter face. The hardness of the pure copper and CAB0 was noticed as 65 $HV_{0.1}$ and 120 $HV_{0.1}$ respectively. The addition of 2 wt % H_3BO_3 in Cu matrix decreases the hardness of the developed composite (CAB2) to 102 $HV_{0.1}$. However, the addition of 4 wt % H_3BO_3 in Cu matrix further lessen the hardness of the developed composite (CAB4) and attained the value 83 $HV_{0.1}$. The mix of 2 wt % H_3BO_3 significantly reduced the coefficient of friction (COF) and the developed composite (CAB2) attained the lowest friction coefficient and wear rate across all testing loads. The favorable lubricity attained by the formulated composite (CAB2) is due to addition of optimal (2 wt %) of H_3BO_3 which develops lubricating phases i.e. $Al_4B_2O_9$ and B_2O_3 in between the mating surfaces and avoid metal to metal contact. The synergistic effect of Al_2O_3 and boric acid in the formulated composite (CAB2) and the development of aluminum borate ($Al_4B_2O_9$) minimized the direct contact and hence improved tribo performance.
71.	Tailoring the properties of WO_3 via 120MeV Ni^{7+} beam irradiation: A pathway to high-performance hydrogen sensor AK Verma, C Prakash…**VKSingh**… - Chemical Engineering Journal, 2025 **Abstract:** The development of high-performance hydrogen sensors is essential for several industrial and environmental applications. The 120 MeV Ni^{7+} Swift heavy ion beam with a

	fluence of 1×10^{13} ions/cm^2 irradiated spin-coated WO_3 thin films. The irradiated WO_3 film was studied for hydrogen gas sensing at an optimized temperature. Characterization techniques, including XRD, Raman, AFM, FESEM, UV–Vis, and FTIR, were employed to analyze optical, morphological, and structural characteristics of pre- & post-irradiated thin films. The crystallite size was reduced from 39.8 to 26.2 nm, and no phase change occurred after the irradiation. The reduced peak intensity obtained from the XRD pattern revealed a reduction in crystallinity. The reduced intensity in Raman peaks validated XRD results by pointing to the decrease in crystallinity. Post irradiation, the energy transfers from the strong Ni^{7+} ion beam to the lattice through electron-phonon coupling (electronic energy loss) causing the surface roughness to rise. The nano-cuboidal-like structures of the pristine film showed structural distortion post-irradiation. The relative sensing response for irradiated film compared to pristine film improved from 45.02% to 67.70% with exposure to the 75 ppm hydrogen gas concentration at 100°C . The recovery and response time significantly improved for the irradiated film. The results indicate that ion beam irradiation is a feasible method for enhancing WO_3-based hydrogen sensors, facilitating the development of next-generation gas sensing systems with enhanced performance.
72.	The strong spectral-and time-dependent emission of NV center charge state in bulk diamonds **A Redhu, R Dhankhar,** S Dey, **RV Nair** - Journal of Applied Physics, 2025 **Abstract:** We discuss charge state ratio-dependent spectral and temporal emission properties of nitrogen-vacancy (NV) centers in bulk diamonds. An understanding of the charge state ratio in artificially grown diamonds is important to design them for NV-based magnetometry. We show that the NV charge state ratio strongly correlates with the intensity of the zero-phonon line (ZPL) of NV^-, which is supported by an emission dip at 2.87 GHz in spin-selective optical transitions. The Debye–Waller factor of NV centers depends on the charge state ratio, and it increases for NV^- with an increase in the charge state ratio. We observe that the energy separation between the second phonon sideband (PSB) and ZPL does not scale multiplicatively with that of the energy separation between first PSB and ZPL. This deviation becomes more pronounced with an increase in charge state ratio, suggesting anharmonicity of vibrational energy levels, rather than the usually reported harmonicity. Further, we discuss the inherent relation between decay rates and charge states as a function of emission wavelengths. The excited state lifetime of NV^0 remains constant, whereas the NV^- lifetime decreases with an increase in the charge state ratio, with an overall decrease of 37%. Our results show an emission spectra-based approach to estimate the charge state ratio in diamond crystals, which is helpful for quantum-enhanced sensing and magnetometry.
73.	Third-order nonlinear optical modulation in MoS_2 nanosheets in the presence of CdSe and CdSe/V_2O_5 quantum dots **SR Konda**, P Barik, S Singh… - Advanced Optical Materials, 2025 **Abstract:** Embedding semiconductor quantum dots (QDs) into a 2D transition metal dichalcogenide (TMDCs) can significantly modulate the electronic charge transfer and, hence, the nonlinear optical (NLO) properties of the TMDCs. However, the influence of strong interactions within 2D nanostructure-QDs composites on their third-order NLO responses has not been explored thus far. The third-order NLO characteristics of few-layered MoS_2 nanosheets embedded with CdSe and CdSe/V_2O_5 QDs are studied using 35-fs pulses at 400 and 800 nm excitations. It is observed that an alteration of the third-order NLO properties in MoS_2 occurs in the presence of QDs. Notably, the MoS_2-QDs hybrid system exhibits a significant modulation in third-order nonlinearities, with a substantial multi-fold increase in the figure of merit in the presence of core CdSe QDs and suppression with passivated CdSe/V_2O_5 QDs. These findings strongly indicate that QD-based hybrid systems with charge transfer channels probably enhance carrier mobility and enable tunable electron transfer dynamics, which can emerge as a viable strategy for tailoring third-order NLO properties in TMDCs, positioning these hybrid materials as promising candidates for optoelectronic applications.

74.	WIND: A wireless intelligent network digital twin for federated learning and multi-layer optimization SK Singh… **B Kumbhani, S Darshi** - IEEE Communications Standards Magazine, 2025 **Abstract:**The forthcoming wireless network is expected to support a wide range of applications, from supporting autonomous vehicles to massive Internet of Things (IoT) deployments. However, the coexistence of diverse applications under a unified framework presents several challenges, including seamless resource allocation, latency management, and systemwide optimization. Considering these requirements, this paper introduces WIND (Wireless Intelligent Network Digital Twin), a self-adaptive, self-regulating, and self-monitoring framework that integrates Federated Learning (FL) and multi-layer digital twins to optimize wireless networks. Unlike traditional Digital Twin (DT) models, the proposed framework extends beyond network modeling, incorporating both communication infrastructure and application-layer DTs to create a unified, intelligent, and context-aware wireless ecosystem. Besides, WIND utilizes local Machine Learning (ML) models at the edge node to handle low-latency resource allocation. At the same time, a global FL framework ensures long-term network optimization without centralized data collection. This hierarchical approach enables dynamic adaptation to traffic conditions, providing improved efficiency, security, and scalability. Moreover, the proposed framework is validated through a case study on federated reinforcement learning for radio resource management. Furthermore, the paper emphasizes the essential aspects, including the associated challenges, standardization efforts, and future directions opening the research in this domain.

Disclaimer: This publication digest may not contain all the papers published. Library has compiled the publication data as per the alerts received from Scopus and Google Scholar for the affiliation “Indian Institute of Technology Ropar” for the month of June, 2025. The author(s) are requested to share their missing paper(s) details if any, for the inclusion in the next publication digest.